

Chaos and complexity of quantum motion

This article has been downloaded from IOPscience. Please scroll down to see the full text article.

2007 J. Phys. A: Math. Theor. 40 7881

(<http://iopscience.iop.org/1751-8121/40/28/S02>)

View [the table of contents for this issue](#), or go to the [journal homepage](#) for more

Download details:

IP Address: 171.66.16.109

The article was downloaded on 03/06/2010 at 05:19

Please note that [terms and conditions apply](#).

Chaos and complexity of quantum motion

Tomaz Prosen

Physics Department, Faculty of mathematics and physics, University of Ljubljana, Jadranska 19, SI-1000 Ljubljana, Slovenia

Received 15 February 2007, in final form 18 April 2007

Published 27 June 2007

Online at stacks.iop.org/JPhysA/40/7881

Abstract

The problem of characterizing the complexity of quantum dynamics—in particular of locally interacting chains of quantum particles—will be reviewed and discussed from several different perspectives: (i) stability of motion against external perturbations and decoherence, (ii) efficiency of quantum simulation in terms of classical computation and entanglement production in operator spaces, (iii) quantum transport, relaxation to equilibrium and quantum mixing, and (iv) computation of quantum dynamical entropies. Discussions of all these criteria will be confronted with the established criteria of integrability or quantum chaos, and sometimes quite surprising conclusions are found. Some conjectures and interesting open problems in ergodic theory of the quantum many problem are suggested.

PACS numbers: 05.45.Pq, 05.45.Jn, 03.67.Mn, 05.60.Gg

(Some figures in this article are in colour only in the electronic version)

1. Introduction

This paper will discuss the possibilities of characterizing *randomness* and *dynamical complexity* in quantum mechanics and relating this issue to the questions of non-equilibrium statistical mechanics. We shall try to illustrate, mainly by presenting various numerical examples, a possible ‘cyclist approach’ [1] towards the *quantum many-body problem* which is inspired by experiences gained in studies of quantum and classical chaos of one or few particles (see e.g. [1, 2]).

Solving the many-body problem in quantum mechanics presented a major challenge from its very beginnings. And along the way, many ingenious important analytical and efficient numerical methods of solution have been developed, for example Bethe ansatz [3], later generalized and interpreted as the quantum inverse scattering problem [4], real space renormalization group methods [5], quantum Monte Carlo [6], density-matrix renormalization group (DMRG) [7], and more recently various quantum information-theoretic-based time-dependent DMRG (tDMRG) [8–10]. The ultimate aim of any of these methods is to efficiently

find analytical or numerical approximation to the solution for some of the physical observables in the quantum many-body problem; however, many methods work only under some specific conditions which are not always well understood. For example, Bethe ansatz and quantum inverse scattering work only for a small subset of problems which are *completely integrable*, and which may often have very non-generic non-equilibrium properties, such as e.g. ballistic transport at high temperatures [11]. Quantum Monte Carlo techniques represent a very successful set of numerical methods which can yield thermodynamic equilibrium averages for generic (non-integrable) systems, however they are practically useless for computing non-equilibrium, or time-dependent quantities, such as transport coefficients. A traditional DMRG method [7] is provably very successful for computing accurate ground state expectation values of almost any physical observables of one-dimensional interacting systems. And tDMRG [8, 10] promised to extend the success of DMRG to time-dependent physics. Indeed, the first numerical experiments looked very promising, but after a closer look one may realize that they have all been applied to a rather special subset of interacting systems and to a rather special subset of initial states. For generic (non-integrable) interacting systems or for sufficiently complex initial states, tDMRG should fail to provide an efficient computation as shall be discussed below. In our view, this is to be expected, and represents an intrinsic characteristic of quantum complexity of such system and should correspond to many-body extensions of the phenomena of quantum chaos [2] where spectra and eigenvector coefficients can be described by statistical ensembles of random matrices. In the past two, almost three decades there has been a lot of activity in the so-called field of quantum chaos, or quantum chaology [12], where people were trying to understand the essential and significant features of quantum systems which behave chaotically in the classical limit. Classical chaos can be defined in terms of positive (algorithmic, Kolmogorov–Chaitin) complexity of systems' orbits. Still, the question whether such definition of complexity can be in an intuitively sensible way translated to quantum mechanics failed to be answered in spite of many efforts. It seems that quantum systems of finite (one or few body) chaotic systems are generically more robust against imperfections [13] than their classical counterparts, which is consistent with a simple illustration based on wave-stability of unitary quantum time evolution [14].

Nevertheless, it has been suggested that exponential sensitivity to initial conditions, the essential characteristics of classically chaotic systems, has many fingerprints in quantum mechanics. For example, in one of the pioneering works on quantum Loschmidt echoes (or fidelity decay), Jalabert and Pastawski [15] have shown that in the semi-classical regime, decay of system's sensitivity to external perturbation, as defined by fidelity, is exponential with the rate which can be related to classical Lyapunov exponents. However, this is only true in sufficiently semi-classical regime, where the effective Planck constant is smaller than the effective strength of perturbation, and where fidelity can be essentially explained classically [16]. On the other hand, in purely quantum regimes, quantum fidelity decays in completely different manner than the classical fidelity, and quite surprisingly displays slower decay for systems with stronger decay of temporal correlations [13].

Throughout this paper we shall discuss various ergodic properties of a simple toy model of non-integrable interacting quantum many-body system, namely kicked Ising (KI) chain [17], and its time-independent version, which (both) undergo a transition from integrable to quantum chaotic regimes when the direction of the (kicking) magnetic field is changed. By simulating the dynamics of the model in terms of tDMRG, we find that it can be performed efficiently only in the integrable regimes. Being interested in statistical mechanics of the model we shall describe numerical experiments addressing the questions on the relationship between the onset of quantum chaos in the KI model and its quantum mixing property, namely the nature of relaxation to equilibrium, and the properties of a non-equilibrium steady state. On

one hand, we argue that the regime of quantum chaos essentially corresponds to the regime of quantum ergodicity and quantum mixing where diffusive transport laws are valid. On the other hand, we conjecture that the transition to non-ergodic regime may occur before the system parameters reach the integrable point (even in thermodynamic limit), and that non-ergodic to ergodic transition can be characterized with order parameters which change discontinuously at a critical value of system parameter. We argue that the process of relaxation to equilibrium in a quantum chaotic (mixing) case can be described in terms of quantum analogues of Ruelle resonances [18]. Furthermore, we conjecture that the eigenvectors of this process possess a certain scale invariance which can be described by simple power laws. We also discuss a possibility of numerical calculation of quantum dynamical entropies [19–21] in a non-trivial setting of the KI model, and find, quite remarkably, that positivity of such dynamical entropies *does not correspond* to any other measures of quantum chaos, namely quantum dynamical entropies appear to be positive even in the integrable regimes.

About two thirds of the material presented in this paper constitutes a review of a selection of recent results related to quantum chaos in many-body systems, with a flavour of quantum information. However, about one third of the material, constituting a major part of section 7, is new and original and has not yet been published before. The paper is organized as follows. In short section 2, we review basic definitions of complete integrability and quantum chaos, in particular in the context of many-body systems. In section 3, we introduce the KI model which will serve us as a very convenient and efficient toy model to numerically demonstrate all the phenomena discussed in this paper. In section 4, we discuss the robustness of quantum systems to external perturbations and decoherence in open quantum systems, mainly as characterized by quantum Loschmidt echoes and entanglement between the system and the environment. In section 5, we discuss the time efficiency of best (known) classical simulation, namely using tDMRG, of locally interacting 1D quantum systems and its possible dependence on integrability of the model. In section 6, we relate standard criteria of quantum chaos to normal (diffusive) versus anomalous (ballistic) transport and discuss a simulation of a quantum heat current in a non-equilibrium steady state. In section 7, we discuss a problem of quantum relaxation to equilibrium, i.e. the quantum mixing property, and quantitative characterization of quantum dynamical complexity. This section contains a large portion of original intriguing numerical results which support few interesting and perhaps surprising conjectures. In section 8, we conclude and discuss some open problems.

2. Integrability versus chaos

The central issue of this paper is to verify and demonstrate to what extent the *complete integrability* affects non-equilibrium properties of quantum many-body systems and their dynamical complexities, and conversely, whether (*strong*) *non-integrability* generically coincides with the established criteria of *quantum chaos*.

Let us start by giving some established definitions (see e.g. [1, 2, 4, 22]) of the basic terms needed to understand the issue.

A classical Hamiltonian many-body system with L degrees of freedom is *completely integrable*, if there exist L functionally independent global smooth phase-space functions (integrals of motion) which are mutually in involution, i.e. all Poisson brackets among them vanish. In such a case, global canonical transformation to canonical *action-angle* variables can be constructed, and dynamics can be explicitly solved—at least in principle. For locally interacting *infinite* systems, ($L \rightarrow \infty$) analytic methods for an explicit construction of integrals

of motion and canonical action-angle variables are known which usually go under a common name of the *inverse scattering method*. An explicit solution by a mapping to an iso-spectral Schrödinger problem in terms of an inverse scattering technique is usually understood as a definition of *complete integrability* in such context.

The definition of *quantum complete integrability* is less unique. Nevertheless, algebraic, non-commutative versions of the inverse scattering technique exist and can be applied to some quantum interacting lattices in one dimension, generalizing the famous Bethe ansatz solution of the Heisenberg spin-1/2 chain, and this is used as the most general known definition of *quantum complete integrability*. Other versions of integrability for finite L quantum systems have been proposed but they do not correspond to the integrability of the underlying classical limit, if the latter exists, so these ideas will not be considered in this paper.

It has not been generally accepted yet, though demonstrated in many occasions, that completely integrable quantum systems constitute only a small subset of physical models and possess many exceptional (non-generic) non-equilibrium dynamical properties, such as for example anomalous transport at finite temperatures (see e.g. [11].)

On the other extreme of ergodic hierarchy, we have chaotic systems. In classical Hamiltonian dynamics of few particles, chaos is best defined in terms of positive algorithmic (Kolmogorov) complexity of systems' trajectories, or equivalently, by exponential sensitivity to initial conditions. However, bounded quantum systems of a finite number of particles cannot be dynamically complex as their excitation spectrum is discrete, and hence the evolution is necessarily quasi-periodic (or almost periodic). Still, quite surprisingly, even for such systems certain dynamical properties are *random* and *universal*, if the underlying classical limit is sufficiently strongly chaotic [2, 12]. But genuine dynamical complexity may emerge in the thermodynamic limit. However, there is still no completely satisfactory definition of dynamical chaos for infinite quantum systems. The commonly used working definition is the reference with the *random matrix theory* [2], namely the many-body quantum system is said to be quantum chaotic if its excitation spectrum or some other dynamical properties can be (on certain energy, or time scale) well described by ensembles of random Hermitian matrices with appropriate symmetry properties.

3. Toy model

Throughout this paper we shall use, either for the illustration of theoretical results, or for numerical experimental studies, the following 1D locally interacting quantum lattice system, namely a chain of L qubits, or spin-1/2 particles, coupled with nearest neighbour Ising interaction and periodically kicked with a spatially homogeneous, but *arbitrarily oriented* magnetic field. In a suitable dimensionless units, our model can be written in terms of a three-parameter periodic time-dependent Hamiltonian

$$H(J, h_x, h_z; t) = \sum_{j=0}^{L-1} \{J\sigma_j^x \sigma_{j+1}^x + \delta_p(t)(h_x \sigma_j^x + h_z \sigma_j^z)\}. \quad (1)$$

$\delta_p = \sum_{m \in \mathbb{Z}} \delta(t - m)$ is a unit-periodic Dirac delta and $\sigma_j^{x,y,z}$ are the usual Pauli spin variables on a finite lattice $j \in \mathbb{Z}_L = \{0, 1, \dots, L-1\}$, satisfying the commutation (Lie) algebra $[\sigma_j^\alpha, \sigma_k^\beta] = \sum_\gamma 2i\varepsilon_{\alpha\beta\gamma} \delta_{jk} \sigma_j^\gamma$. Sometimes it will turn fruitful if we extend the set of Pauli matrices by identity matrix and assign them a numerical superscript $\sigma_j^\alpha, \alpha \in \mathbb{Z}_4$, namely $\sigma_j^0 \equiv \mathbf{1}, \sigma_j^1 \equiv \sigma_j^x, \sigma_j^2 \equiv \sigma_j^y, \sigma_j^3 \equiv \sigma_j^z$. The finite chain will often be treated with *periodic boundary conditions*, $\sigma_L^\alpha \equiv \sigma_0^\alpha$, and sometimes the thermodynamic limit (TL) $L \rightarrow \infty$ will be considered, in particular when we shall study the statistical mechanics of (1) in section 7.

Although kicked Hamiltonian one-particle models have been very popular in the field of nonlinear dynamics and quantum chaos for decades, for example Chirikov's kicked rotator model [23], the use of kicked systems in quantum many-body physics has been so far very limited. If one is not only interested in zero temperature (ground state) or low temperature physics, then as we shall try to demonstrate in this review, kicked many-body models like (1) provide simpler and clearer phenomenological picture of global dynamics than time-independent models. The main reason is that since energy is not a conserved quantity, the entire Hilbert space of many-body configurations is accessible for non-integrable dynamics, and the notions of quantum ergodicity and mixing (see e.g. [24] for definitions and further references) can be defined more clearly than in the time-independent, autonomous setting. Perhaps the first kicked interacting quantum lattice has been introduced in [25]. Even if in traditional solid state physics such kicked dynamics would represent unphysically strong excitations, one has to realize that kicked quantum chains could be attractive options as benchmark models of quantum state manipulation and quantum computation in optical lattices.

The *kicked Ising* (KI) model (1) has been defined for the first time in [17], generalizing the integrable KI model with the transverse field introduced in [26]. Clearly, as shown there [26] for the case of the *transverse* field, $h_x = 0$, the time-dependent model (1) can be considered *completely integrable* since it can be solved explicitly, for example by Wigner–Jordan–Bogoliubov transformation to non-interacting spinless fermions, and a large class of its time correlation functions can be calculated explicitly. In addition, an infinite sequence of local conserved quantities (integrals of motion) can be constructed in such a case. There is another, trivial *completely integrable* regime of the KI model, namely the case of the *longitudinal* field, $h_z = 0$. Yet another, more non-trivial *completely integrable* regime of the KI model is found when the magnitude of the dimensionless field is a multiple of $\pi/2$, namely $h = \sqrt{h_x^2 + h_z^2} = n\pi/2, n \in \mathbb{Z}$, since then the magnetic kick can be considered as a multiple of π rotation, and generated by a slightly obscure set of non-interacting spinless fermions.

However, in a general case of the titled magnetic field when both components h_x and h_z are non-vanishing, and $2h/\pi$ is non-integer, the model is non-integrable, and is conjectured to be not amenable to exact analytical methods. As discussed in the following sections, the non-integrable KI model can display a variety of regimes according to the criteria of quantum chaos, quantum ergodicity and quantum mixing. In fact, recently the spectral statistics of the KI model in a strongly non-integrable regime has been studied in detail, and random matrix behaviour has been clearly confirmed at short energy ranges [27].

Due to the kicked nature of interaction, the evolution propagator of the KI model for one unit period of time (the so-called Floquet operator), starting just before the kick, can be constructed explicitly in terms of a time-ordered product

$$U(J, h_x, h_z) = \mathcal{T} \exp \left(-i \int_0^1 dt H(J, h_x, h_z; t - 0) \right) \quad (2)$$

$$= \exp \left(-iJ \sum_j \sigma_j^x \sigma_{j+1}^x \right) \exp \left(-i \sum_j (h_x \sigma_j^x + h_z \sigma_j^z) \right) \quad (3)$$

$$= \prod_j U''_{j,j+1}(J) \prod_j U'_j(h_x, h_z). \quad (4)$$

The last line suggests a simple efficient quantum protocol to simulate the KI model in terms of simple 1-qubit $U'(h_x, h_z) = \exp(-i(h_x \sigma^x + h_z \sigma^z))$ and 2-qubit $U''(J) = \exp(-iJ \sigma^x \otimes \sigma^x)$

quantum gates. If we write a compact kicked Ising 2-qubit gate

$$W(J, h_x, h_z) = U''(J) \cdot (U'(h_x, h_z) \otimes \mathbb{1}) \quad (5)$$

and introduce a left-to-right ordered operator product, namely $\prod_j^+ A_j \equiv \cdots A_1 A_2 A_3 \cdots$, then we can write KI protocol as a simple string of W gates

$$U(J, h_x, h_z) = \prod_j^+ W_{j,j+1}(J, h_x, h_z). \quad (6)$$

The KI model has a better known autonomous limit, namely time-independent Ising chain in a tilted magnetic field

$$H'(J, h_x, h_z) = \lim_{\tau \rightarrow 0} \frac{1}{\tau} \overline{H(\tau J, \tau h_x, \tau h_z; t)} = \sum_j (J \sigma_j^x \sigma_{j+1}^x + h_x \sigma_j^x + h_z \sigma_j^z), \quad (7)$$

which is again non-integrable unless the field is transverse $h_x = 0$, or longitudinal $h_z = 0$.

4. Decoherence and fidelity

4.1. Loschmidt echoes

One of the central questions about the dynamics of complex quantum systems is their robustness against small imperfections in the Hamiltonian. While it is clear that due to unitarity the quantum evolution is stable against variation of initial states [14], it is not so clear how stable it is against variation of the Hamiltonian, either being static or time-dependent—perhaps even noisy.

Let us write the Hamiltonian as $H_\delta = H_0 + \delta V$, where H_0 is the unperturbed Hamiltonian, V is a Hermitian perturbation operator and δ is a small perturbation parameter. Peres [28] proposed the following measure of stability of quantum evolution. Let us start from some fixed initial state $|\psi\rangle$, and write the time evolutions of this state generated with the unperturbed and perturbed Hamiltonian, as $|\psi_0(t)\rangle = U_0(t)|\psi\rangle$ and $|\psi_\delta(t)\rangle = U_\delta(t)|\psi\rangle$, respectively. Then the stability is characterized by fidelity, i.e. the squared overlap between these two states

$$F(t) = |\langle \psi_0(t) | \psi_\delta(t) \rangle|^2 = |\langle \psi | U_0^\dagger(t) U_\delta(t) | \psi \rangle|^2. \quad (8)$$

There are two alternative interpretations of quantum fidelity. (i) One can interpret (8) as a *quantum Loschmidt echo*, namely the probability that the initial state $|\psi\rangle$, which is propagated forward with perturbed evolution $U_\delta(t)$, and after that propagated backwards in time with unperturbed evolution $U_0^\dagger(t) = U_0(-t)$, is again measured in the same (initial) state. Alternatively (ii) is just the square modulus of the expectation value of the unitary echo operator $U_0(-t)U_\delta(t)$ which is the quantum propagator in the *interaction picture*.

There have been three main theoretical approaches to understand the fidelity decay in quantum dynamical systems.

4.1.1. Semi-classical approach. In a seminal work Jalabert and Pastawski derived quantum Loschmidt echo for systems which possess a well-defined classical limit. They have shown that under certain conditions, namely that the perturbation strength is large enough—typically larger than the appropriately scaled Planck constant, and that initial states have certain classical interpretations—such as coherent states, position states, etc, the quantum Loschmidt echo decays exponentially

$$F(t) \sim \exp(-\lambda t), \quad (9)$$

with the rate λ which is *perturbation independent* and typically equals the Lyapunov exponent of the underlying classical dynamics. More recently a completely classical interpretation of this so-called Lyapunov decay has been given [16] in terms of *the classical Loschmidt echo*, and a theory for exponents λ has been developed in terms of the full spectrum of Lyapunov exponents for classical dynamical systems with few [16] or many [29] degrees of freedom.

4.1.2. *Time-dependent perturbation theory and linear response approximation.* In the opposite regime, where the scaled Planck constant is bigger than the perturbation strength δ , one can use time-dependent quantum perturbation theory to second order to derive a simple linear response formula for fidelity decay [13, 17]

$$F(t) = 1 - \frac{\delta^2}{\hbar^2} \int_0^t dt' \int_0^{t'} dt'' C(t', t'') + \mathcal{O}((\delta/\hbar)^4) \tag{10}$$

in terms of a two-point time correlation function of the perturbation

$$C(t', t'') = \langle \tilde{V}(t') \tilde{V}(t'') \rangle - \langle \tilde{V}(t') \rangle \langle \tilde{V}(t'') \rangle, \tag{11}$$

where $\tilde{V}(t) = U_0(-t)VU_0(t)$ is the perturbation operator in the interaction picture and $\langle \cdot \rangle = \langle \psi | \cdot | \psi \rangle$ is an expectation value in the initial state.

From this formula, which can be viewed as a kind of Kubo-like linear response theory for dissipation of quantum information, an interesting conclusion can be drawn. Fidelity decays faster for systems with slower decay of temporal correlations, or an alternatively phrased, quantum system is more robust against external perturbations if it relaxes to equilibrium faster.

One can actually go beyond the second-order perturbation theory, and sum up the Born series for fidelity to all orders in many specific situations [13]. Since we are here mainly interested in qubit (spin-1/2) chains, we shall only review specific results for kicked Ising chain [17]. We shall discuss three different specific values of system parameters; in all three we take $J = 1.0$, $h_z = 1.4$: (a) integrable regime of the transverse field $h_x = 0$, (b) weakly non-integrable regime with $h_x = 0.4$, and (c) strongly non-integrable regime with $h_x = 1.4$. All the results, correlation functions and fidelity, are for random initial states, which can be interpreted as pure states of maximum quantum information, and averaging over random states is equivalent to a tracial state $\langle \cdot \rangle = 2^{-L} \text{tr}(\cdot)$. We consider the evolution operator (2) and perturb it by changing the magnetic field such that the perturbation is generated by the transverse component of the magnetization $M = \sum_j \sigma_j^z$, namely $U_\delta(t) = [U(J, h_x, h_z) \exp(-i\delta M)]^t$.

In the integrable case, or in general, in the non-ergodic case, where the correlation function $C(t', t'') = \langle M(t')M(t'') \rangle$ (note that $\langle M(t) \rangle \equiv 0$) approaches a non-vanishing plateau value as $|t' - t''| \rightarrow \infty$, namely time-averaged fluctuation of magnetization $D_M = \lim_{t \rightarrow \infty} (1/t^2) \int_0^t dt' \int_0^t dt'' C(t', t'')$ is non-vanishing $D_M \neq 0$, one can sum up Born series to all orders, yielding a Gaussian decay of fidelity

$$F(t) = \exp(-(t/\tau_{\text{ne}})^2), \quad \tau_{\text{ne}} = D^{-1/2} \delta^{-1}. \tag{12}$$

The only assumptions are that t is long enough for the time average in the definition of D_M to converge, and short enough that fidelity is still above the finite size plateau value $F^* \sim 1/2^L$. Note that D_M can be considered as an analogue of Drude weight or charge stiffness in the linear response solid state transport theory (see e.g. [11]). In figures 1(a), (b) and 2(a), (b) one can observe the correlation plateaus of correlation functions for integrable and weakly non-integrable cases and respective good agreement with a Gaussian decay of fidelity (12). Note that in the integrable case, the correlation function and the plateau D_M have been also calculated analytically [26]. Note that for comparing different lattice sizes L a size-scaled value of the perturbation strength $\delta' = \delta \sqrt{L/L_0}$, with $L_0 = 24$, has been fixed rather than δ itself.

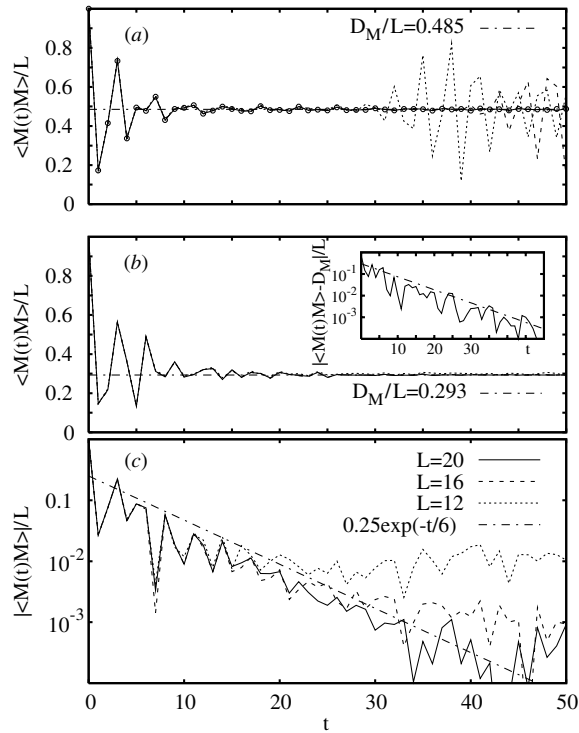


Figure 1. Correlation decay for three cases of a finite KI model: (a) integrable $h_x = 0$, (b) intermediate $h_x = 0.4$ and (c) ergodic $h_x = 1.4$, whereas $J = 1.0$, $h_z = 1.4$, and for different sizes $L = 20, 16, 12$ (solid-dotted connected curves, almost indistinguishable in (a, b)). Circles in (a) show the exact result for $L = \infty$.

On the other hand, for sufficiently strong integrability breaking, say in case (c) of the KI model, the correlation function $C(t' - t'') = C(t', t'')$ decays to zero in TL, which can be interpreted as quantum mixing behaviour. It has been found that quantum mixing behaviour typically corresponds to random matrix (quasi)energy level statistics; see e.g. [24] and the subsequent sections of the present paper. We shall call such behaviour the regime of quantum chaos. Here again, Born series for fidelity can be summed up to all orders, yielding an exponential decay [17]

$$F(t) = \exp(-t/\tau_m), \quad \tau_m = 1/(2\sigma\delta^2), \quad (13)$$

where $\sigma = \int_0^t C(t') dt'$ is a transport coefficient. The assumptions for validity of (13) are that t is larger than a characteristic mixing time scale on which $C(t)$ decays and short enough so that finite size effects in the quantum correlation function $C(t)$ do not yet affect the transport coefficient σ . This regime of fidelity decay is sometimes referred to as the Fermi Golden Rule regime. Again, as demonstrated in figures 1(c) and 2(c), the agreement of numerical data for the KI model with the theory is excellent.

Note that decay time of fidelity scales as $\propto \delta^{-2}$ for ergodic and mixing dynamics, and as $\propto \delta^{-1}$ for non-ergodic dynamics, making the latter much more sensitive to small perturbations.

4.1.3. Random matrix theory (RMT). Complex quantum systems can often be well described by statistical ensembles of Hamiltonians [30]. Assuming that H_0 and V both belong to

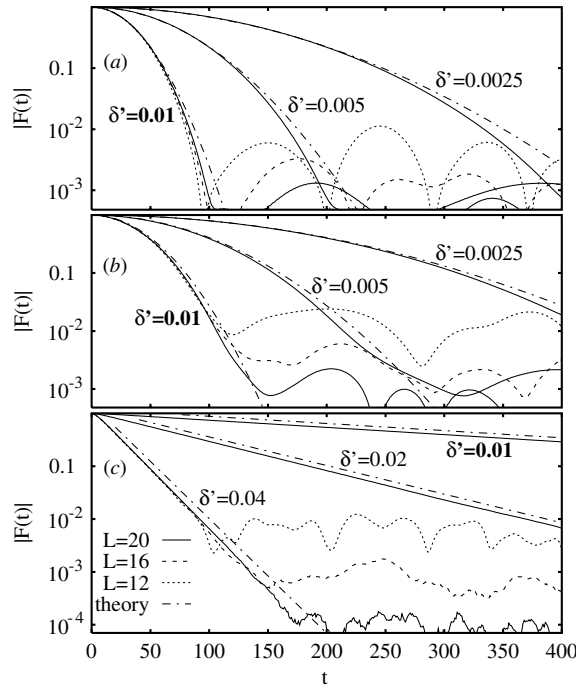


Figure 2. Average fidelity amplitude (absolute value of it) for three cases of finite KI: (a) integrable $h_x = 0$, (b) intermediate $h_x = 0.4$ and (c) ergodic $h_x = 1.4$, whereas $J = 1.0$, $h_z = 1.4$, and for different sizes $L = 20, 16, 12$, and different scaled perturbations δ' . Chain curves give theoretical predictions [13, 17].

canonical ensembles of Gaussian random matrices, one can evaluate ensemble averages of the fidelity and relate $C(t)$ to the spectral form factor of the underlying random matrix ensemble. The perturbative (linear response) theory has been developed in [31], see also [32, 33]. Furthermore, a non-perturbative (super-symmetric) averaging has been successfully applied to obtain exact expressions for average fidelity amplitude in the most interesting cases [34]. RMT theory of fidelity has been successfully applied to chaotic quantum systems and even to several experimental situations [35].

Following more applied philosophy, groups from Toulouse and Como have performed a series of numerical experiments [36] analysing the robustness of several reasonable models of quantum computer hardware under small imperfections, being either due to (static) unwanted inter-qubit coupling or due to stochastic (noisy) unwanted coupling to the environment, when performing quantum algorithms simulating various toy models of classical and quantum single-particle chaos [33], such as for example quantum kicked rotator [37]. The numerical results are in line with a general linear response theory, stating that static perturbations are, in general, more dangerous than noisy ones.

4.2. Decoherence and entanglement between weakly coupled systems

Similar thinking as in the previous subsection can be applied to perhaps even more fundamental problem of quantum physics, to the problem of decoherence [38]. Here we shall limit ourselves to an abstract unitary model of decoherence, where we treat a complete unitary evolution over two subsystems, a central system C and an environment E, and then address a relevant

information about the central system (i.e. the part of the system which is of physical interest) by partially tracing over the environment.

Such a discussion can indeed be followed with a close link to the problem of Loschmidt echoes, by writing the total Hamiltonian $H_\delta = H_0 + \delta V$ as an ideal (unperturbed) separable evolution $H_0 = H_C \otimes \mathbb{1}_E + \mathbb{1}_C \otimes H_E$ perturbed by a small coupling V between the system and the environment. We shall also assume that we start from an initial pure state which is a product state $|\psi\rangle = |\psi_C\rangle \otimes |\psi_E\rangle$. We are interested in the properties of a generally mixed state of the central system obtained by partial tracing over the environment

$$\rho_C(t) = \text{tr}_E [U_\delta(-t)|\psi\rangle\langle\psi|U_\delta(t)]. \quad (14)$$

Then, under an ideal evolution, the state of the system remains a product state at all times, so the state of the central system remains pure and there is no decoherence. Decoherence is usually characterized in terms of decaying off-diagonal matrix elements of ρ_C in a suitable pointer state basis, for example in the eigenbasis of the central system Hamiltonian H_E . In fact for certain special forms of the perturbation operator V , the magnitudes of off-diagonal matrix elements of ρ_C can be literally written as fidelities, or quantum Loschmidt echoes, in the evolution of the environment perturbed by system–environment coupling [39]. In such a framework, the Lyapunov regime of fidelity decay corresponds exactly to the Lyapunov growth of decoherence discussed by Zurek and Paz [40].

However, another interesting indicator of decoherence is the growth of *bi-partite entanglement* between the system and the environment. Perhaps this notion is even more general, since it does not depend on a particular choice of the pointer state basis. Since the state of the universe (central system + environment) is always pure, the characterization of entanglement is easy, say in terms of Von Neuman entropy of ρ_C , $S(t) = -\text{tr}_C \rho_C \log \rho_C$, or linear entropy $S_2(t) = -\log \text{tr}_C \rho_C^2(t)$ which is a negative logarithm of purity $P(t) = \text{tr} \rho_C^2(t)$. Usually, the quantities $S(t)$ and $S_2(t)$ essentially give equivalent results, namely they can both be interpreted as the logarithm of an effective rank of the state ρ_C , but the linear entropy, or purity, is more amenable to analytical calculations.

Again considering chaotic models for the central system and the environment, Miller and Sarkar [41] (see also [42]) have been able to observe the ‘Lyapunov regime’ of entanglement growth, namely $S(t)$ is for sufficiently strong perturbations δ found to grow linearly $S(t) = ht$, with the rate h which is perturbation independent and given by (the sum of positive) classical Lyapunov exponents of the unperturbed, separated (sub)systems.

On the other hand, in the purely quantum regime of small perturbation δ , again typically smaller than the effective Planck constant, one can use time-dependent perturbation theory and derive perturbation-dependent entanglement entropy [43, 44], namely the purity can be explicitly expressed as $P(t) \sim 1 - \delta^2 \mathcal{C}(t)$, where $\mathcal{C}(t)$ is a particular integrated correlation function of the perturbation. In this regime, we again find that quantum systems, and quantum environments, which display faster relaxation to equilibrium, are more robust against decoherence due to typical couplings. For studies of bi-partite entanglement, in particular in the KI model system, see [45, 46].

There exists an even closer connection to fidelity theory, namely one can prove a general inequality [43, 47] stating that purity is always bounded by the square of fidelity

$$(F(t))^2 \leq P(t). \quad (15)$$

In other words, $\log(1/F(t)^2)$ gives an upper bound for the growth of the linear entanglement entropy, $S_2(t) \leq -2 \log F(t)$.

In a slightly different context, *bit-wise* entanglement between a pair of qubits of a quantum register representing a time-dependent quantum state, where the rest of the register

is considered as an environment, has been demonstrated to be an indicator of quantum chaos [48] and even a signature of classical chaos [49].

5. Efficiency of classical simulations of quantum systems

In the theory of classical dynamical systems there is a fundamental difference between integrable and chaotic systems as outlined in section 2. Chaotic systems, having positive algorithmic complexity, unlike the integrable ones, cannot be simulated for arbitrary times with a finite amount of information about their initial states. Computational complexity of individual chaotic trajectories is linear in time; however, if one wants to describe statistical states (phase space distributions) or observables of chaotic classical systems, up to time t , an exponential amount of computational resources is needed, typically $\propto \exp(ht)$, where h is Kolmogorov's dynamical entropy related to exponential sensitivity to initial conditions. But on the other hand, how difficult is it to simulate isolated and bounded quantum systems of many interacting particles using classical resources? In analogy with the classical (chaotic) case, we might expect that the best classical simulation of typical quantum systems (in TL) is exponentially hard, i.e. the amount of computing resources is expected to grow exponentially with time.

Even though there is no exponential sensitivity to initial conditions in quantum mechanics, there is a tensor-product structure of the many-body quantum state space which makes its dimension to scale exponentially with the number of particles, as opposed to linear scaling in the classical case, and due to the presence of entanglement generic quantum time evolution cannot be reduced to (efficient) classical computation in terms of non-entangled (classical-like) states. Here we propose the idea to use *the computation complexity of best possible classical simulation of quantum dynamics, as a measure of quantum algorithmic complexity*. This section essentially reviews the article [50]. We note that our proposal is different from existing proposals of quantum algorithmic complexity [51–54], namely we consider merely the classical complexity of (best) classical simulations of quantum states. In the sense of Mora and Briegel [54], quantum algorithmic complexity *per unit time* of initially simple time-evolving quantum states propagated by locally interacting Hamiltonian H is clearly vanishing, since an approximate quantum circuit which reproduces the state after time t is a simple repetition of Trotter–Suzuki decomposition of $\exp(-iH\delta t)$.

5.1. Time-dependent density-matrix renormalization group: how far can it go?

Recently, a family of numerical methods for the simulation of interacting many-body systems has been developed [8] which is usually referred to as time-dependent density-matrix renormalization group (tDMRG), and which has been shown to provide an efficient classical simulation of some interacting quantum systems. Of course, it cannot be proven that tDMRG provides the best classical simulation of quantum systems, but it seems that it is by now the best method available. Simulations of locally interacting one-dimensional quantum lattices were actually shown rigorously to be efficient in the number L of particles [55] (i.e., computation time and memory resources scale as polynomial functions of L at fixed t , whereas here we are interested in the scaling of computation time and memory with physical time t (in TL, $L = \infty$), referred to as *time efficiency*).

In this section, we address the question of time efficiency implementing tDMRG for a family of Ising Hamiltonian (7) which undergoes a transition from integrable (transverse Ising) to non-integrable quantum chaotic regime as the magnetic field is varied. We mainly consider time evolution in operator spaces [10], say of density matrices of quantum states, or (quasi)

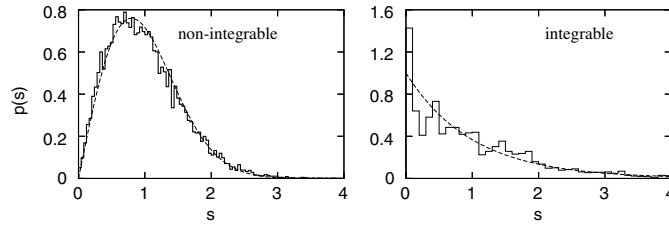


Figure 3. Nearest neighbour LSD for H_C (left) and H_R (right) for $L = 12$. Dashed curves are $p(s) = s\pi/2 \exp(-\pi^2 s^2/4)$ (left) and $p(s) = \exp(-s)$ (right), typical for chaotic and regular systems, respectively [2]. Eigenenergies $\in [-9, 9]$ were used and statistics for even- and odd-parity states were combined.

local operator algebras. Note that time evolution of pure states is often ill defined in TL [56]. As a quantitative measure of time efficiency, we define and compute the minimal dimension $D_\epsilon(t)$ of the matrix product operator (MPO) representation of quantum states/observables which describes time evolution up to time t within fidelity $1 - \mathcal{O}(\epsilon)$. Our main question concerns possible scaling of $D_\epsilon(t)$ for different types of dynamics, and indeed we shall demonstrate a correspondence between, respectively, quantum chaos or integrability, and the exponential or polynomial growth of $D_\epsilon(t)$.

The key idea of operator-valued tDMRG [10] is to represent any operator in a matrix product form,

$$O_{\text{MPO}} = \sum_{s_j} \text{tr}(A_0^{s_0} A_1^{s_1} \cdots A_{L-1}^{s_{L-1}}) \sigma_0^{s_0} \sigma_1^{s_1} \cdots \sigma_{L-1}^{s_{L-1}}, \quad (16)$$

in terms of $4L$ matrices $A_j^{s_j}$ of fixed dimension D . The number of parameters in the MPO representation is $4LD^2$, and for sufficiently large D it can describe any operator. In fact, the minimal D required equals the maximal rank of the reduced super-density matrix over all bi-partitions of the chain. The advantage of MPO representation lies in the fact that doing an elementary local one or two qubit unitary transformation $O' = U^\dagger O U$ can be done locally, affecting only a pair of neighbouring matrices $A_j^{s_j}$.

We will illustrate evolution of the Ising chain (7), with *open* boundary conditions, for two different magnetic field values: (i) an integrable (regular) case $H_R = H'(1, 0, 2)$ with a transverse magnetic field, and (ii) a non-integrable (quantum chaotic) case $H_C = H'(1, 1, 1)$ with a 45° -tilted magnetic field. To confirm that H_C and H_R indeed represent generic quantum chaotic and regular system, respectively, we calculated level-spacing distribution (LSD) of their spectra (shown in figure 3). LSD is a standard indicator of quantum chaos [2]. It displays characteristic level repulsion for strongly non-integrable quantum systems, whereas for integrable systems there is no repulsion due to the existence of conservation laws and quantum numbers. Evolution by tDMRG proceeds as described in [8, 10, 50] using an approximate Trotter–Suzuki factorization, for some time step δt , of the evolution operator $U(t) = \exp(-iHt)$ in terms of 2-qubit gates. And for each 2-qubit gates, the matrices $A_j^{s_j}$ can be updated using a singular value decomposition with some truncation error η . Interestingly, it has been found [50] that the sum of all truncation errors up to time t , denoted by $\eta(t)$ (provided δt is small enough so that the Trotter–Suzuki factorization error is negligible) is simply proportional to the *fidelity error*, namely

$$1 - F(t) \approx c\eta(t)/\delta t, \quad (17)$$

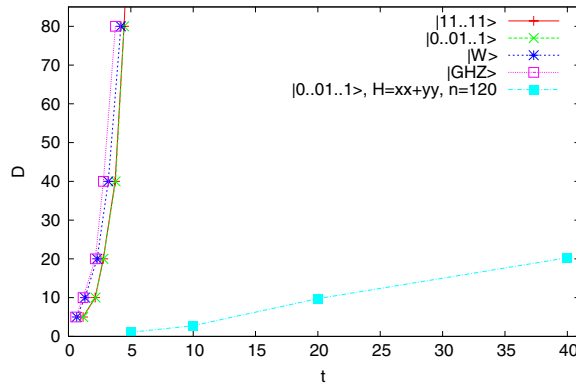


Figure 4. MPS rank $D_\epsilon(t)$ for simulating pure states with the integrable transverse Ising model H_R , except full squares which are for Heisenberg XX chain, starting from the initial states indicated in the legend (explanation: $|W\rangle = (|10\dots 0\rangle + |01\dots 0\rangle + \dots + |00\dots 1\rangle)/\sqrt{L}$ and $|GHZ\rangle = (|00\dots 0\rangle + |11\dots 1\rangle)/\sqrt{2}$). Note that the full squares correspond to the same example as studied in [9].

where

$$F(t) = \frac{|\text{tr}\{O_{\text{MPO}}(t)O_{\text{exact}}(t)\}|^2}{|\text{tr}\{O_{\text{MPO}}^2(t)\}||\text{tr}\{O_{\text{exact}}^2(t)\}|}, \tag{18}$$

and the numerical constant $c \sim 1$ does not depend on either δt , D or L . The central quantity we are going to study is $D_\epsilon(t)$ which is the minimal dimension D of matrices $A_i^{s_j}$ in order for the total truncation error $\eta(t)$ to be less than some error tolerance ϵ , for evolution to time t . In numerical experiments shown, we take $\epsilon = 10^{-4}$ except for simulating thermal states of quenched Hamiltonians where $\epsilon = 10^{-6}$.

5.2. Simulating pure states

For a reference, we start by investigating the evolution of pure states following the basic tDMRG algorithm [8]. We studied time efficiency of simulation of *pure states* in a Schrödinger picture, for which many examples of efficient applications exist, however all for initial states of rather particular structure, typically corresponding to low energy sectors of few quasi-particle excitations or to low-dimensional invariant subspaces. Treating other, typical states, e.g. eigenstates of unrelated Hamiltonians, linear combinations of highly excited states, or states chosen randomly in the many-particle Hilbert space, we found that, irrespectively of integrability of dynamics, tDMRG is *not* time efficient, $D_\epsilon(t)$ typically grows exponentially in time even in the integrable case of the transverse field (consistently with a linear growth of entanglement entropy [57]). Numerical results are summarized in figure 4.

5.3. Simulating local observables

We continue by discussing the time efficiency of the operator-valued tDMRG method using MPOs (16). Let us first study the case where the initial operator is a local operator in the centre of the lattice $O(0) = \sigma_{L/2}^s$, $s \in \{x, y, z\}$. In the integrable case, time evolution $O(t)$ can be computed exactly in terms of Jordan–Wigner transformation and Toeplitz determinants [58]; however, for initial operators with an infinite *index*¹ such as for $\sigma_{L/2}^{x,y}$, $L \rightarrow \infty$, the

¹ The index of a product operator O (section 2, 1st part of [58]) is half the number of Fermi operators in Jordan–Wigner transformation of O and is a conserved quantity for H_R .

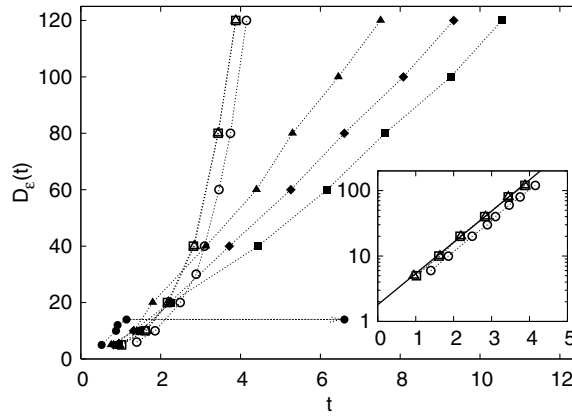


Figure 5. $D_\epsilon(t)$ for local initial operators. We consider three cases $O(0) = \sigma_{L/2}^{x,y,z}$ (empty circles, squares and triangles), for non-integrable evolution H_C , and four cases, $O(0) = \sigma_{L/2}^{x,y}$ (full squares, diamonds), $\sigma_{L/2-1}^z \sigma_{L/2}^y$ (full triangles), all with the infinite index, and $O(0) = \sigma_{L/2-1}^z \sigma_{L/2}^z$ (full circles) with index 2, for integrable evolution H_R . In the inset, we plot the data for the non-integrable case H_C in semi-logarithmic scale, and the full line in the inset illustrates the exponential growth $\propto e^{1.1t}$. Full squares and diamonds are for $L = 40$, otherwise $L = 20$.

evolution is rather complex and the effective number of terms (Pauli group elements) needed to span $O(t)$ grows exponentially in t . In spite of that, our numerical simulations shown in figure 5 strongly suggest the linear growth $D_\epsilon(t) \sim t$ for initial operators with infinite index. Quite interestingly, for initial operators with a *finite* index, $D_\epsilon(t)$ saturates to a finite value, for example $D_\epsilon(\infty) = 4$ for $\sigma_{L/2}^z$, or $D_\epsilon(\infty) = 16$ for $\sigma_{L/2-1}^z \sigma_{L/2}^z$. In non-integrable cases the rank has been found to grow exponentially, $D_\epsilon(t) \sim \exp(h_q t)$ with the exponent h_q which does *not* depend on ϵ , properties of $O(0)$ or L , for large L . For $H = H_C$, we find $h_q = 1.10$.

5.4. Simulating extensive observables

In physics, it is often useful to consider extensive observables, for instance translational sums of local operators, e.g. the Hamiltonian H or the total magnetization $M^s = \sum_{j=0}^{L-1} \sigma_j^s$. As opposed to local operators, extensive initial operators, interpreted as W-like states in the operator space, contain some long-range ‘entanglement’ so one may expect that tDMRG should be somewhat less efficient than for local operators. Indeed, in the integrable case we find for extensive operators with the *finite* index that $D_\epsilon(t)$ does no longer saturate but now grows linearly, $D_\epsilon(t) \sim t$, whereas for extensive operators with the *infinite* index the growth may be even somewhat faster, most likely quadratic $D_\epsilon(t) \sim t^2$ but clearly slower than exponential. In the non-integrable case, we again find exponential growth $D_\epsilon(t) \sim \exp(h_q t)$ with the same exponent $h_q = 1.10$ as for local initial observables. The results are summarized in figure 6.

5.5. Simulating thermal states

In the last set of numerical experiments we consider time efficiency of the evolution of a thermal initial state $O(t) = Z^{-1} \exp(-\beta H_0)$ under a sudden change of the Hamiltonian at $t = 0$, namely $H(t < 0) = H_0 = H'(1, 0, 1)$, $H(t > 0) = H_1$. Again, we treat two situations: in the first case we consider a change after which the Hamiltonian remains integrable, $H_1 = H'(1, 0, 2) = H_R$, while in the other case the change breaks integrability of

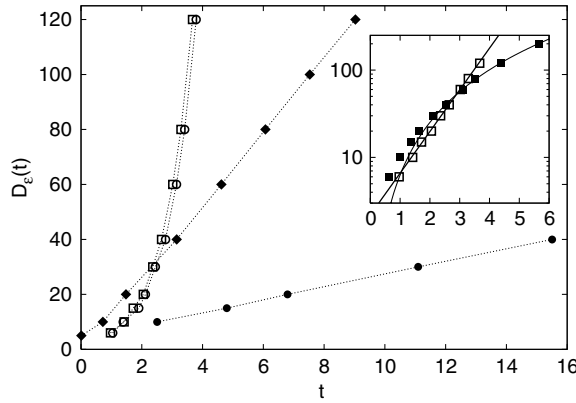


Figure 6. $D_\epsilon(t)$ for extensive initial operators. For both Hamiltonians H_C, H_R we take $O(0) = \sum_j \sigma_j^x$ (empty, full squares) with infinite index, and $O(0) = H'(1, 0, 1)$ (empty, full circles) with index 1. For H_R we also show the case $O(0) = \sum_j \sigma_j^z \sigma_{j+1}^z + \sigma_j^y \sigma_{j+1}^y$ (full diamonds) with index 1 and 2. In the semi-log inset we illustrate exponential increase $\propto e^{1.1t}$ (full straight line) for H_C and polynomial $\sim t^2$ (full curve) for H_R . For full circles $L = 64$, otherwise $L = 32$.

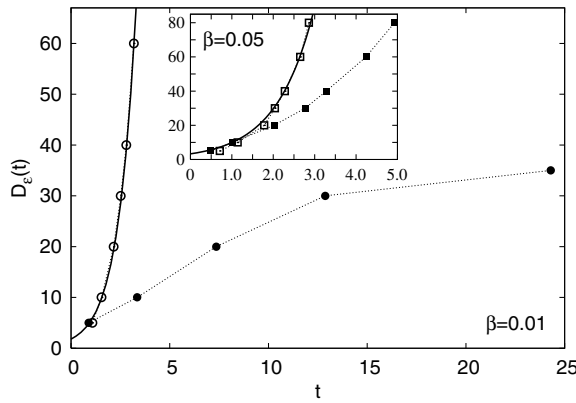


Figure 7. $D_\epsilon(t)$ for thermal states of H_0 with $\beta = 0.01$ ($\beta = 0.05$ in inset), for evolution with H_C (open symbols) and H_R (full symbols) at $L = 40$. Solid curves again indicate exponential increase $\propto e^{1.1t}$.

the Hamiltonian, $H_1 = H'(1, 1, 1) = H_C$. The initial state is prepared by means of imaginary time tDMRG from an initial identity operator using the same MPO rank D as it is later used for real time dynamics. We find, consistently with previous results, that at high temperature ($\beta \ll 1$) the rank $D_\epsilon(t)$ grows very slowly, perhaps slower than linear, in the integrable case, and exponentially $D_\epsilon(t) \sim \exp(h_q t)$, in the non-integrable case. Interestingly, at lower temperatures we find exponential growth in both cases, even in the integrable one. This is not unreasonable as the initial (thermal) state can be expanded in a power series in β and the higher orders H_0^p become less local with a longer entanglement range as we increase the power p . These results are summarized in figure 7.

6. Quantum chaos and far from equilibrium quantum transport

In this section, we would like to demonstrate the connection between quantum chaos, (non)integrability and transport in non-equilibrium steady states of interacting quantum chains [59]. Within the linear response theory, the property of quantum mixing (which is typically implied by quantum chaos, i.e. by the validity of random matrix level statistics [24]; see also correlation functions in section 4) is typically synonymous for normal quantum transport since it implies *finite* Kubo transport coefficients [60] (provided temporal correlation functions decay fast enough).

However, here we would like to address the connection between quantum chaos and transport in a far-from-equilibrium steady state, which may be beyond applicability of linear response. In particular, we are interested in the validity [61] of the Fourier law $J = -\kappa \nabla T$ in quantum chains, relating the macroscopic heat flux J to the temperature gradient ∇T .

To investigate this problem one has to deal with a finite open system connected to heat baths. Here we consider an interacting quantum spin-1/2 chain (7) which exhibits the transition from integrability to quantum chaos as a parameter, e.g. the magnetic field, is varied. The standard treatment of this problem is based on the master equation, thus limiting numerical investigations to relatively small system sizes. By using this method, in an interesting paper [62], the decay of current correlation function in a model of non-integrable chain of quantum spins is computed. However, these results were not fully conclusive and the conclusions rely on linear response theory. Also, in [63] Lindblad formalism was used to study the validity of Fourier's law for different types of spin-spin interaction.

Here we describe a different approach (see [59] for details), namely we follow the evolution of the system described by a *pure* state, which is *stochastically* coupled to an idealized model of heat baths. Stochastic coupling is realized in terms of a local measurement at the boundary of the system and *stochastic* but *unitary* exchange of energy between the system and the bath. By this method we have been able to perform very effective numerical simulations which allow us to observe a clear energy/temperature profile and to measure the heat current J . Again we consider the Ising spin chain in the magnetic field (7) of size L , where the first and the last spin are coupled to thermal baths at temperatures T_l and T_r , respectively. In the non-integrable regime where the spectral statistics is described by RMT—the regime of quantum chaos—we found very accurate Fourier law scaling $J/\Delta T \propto 1/L$, where L is the size of the chain. In the integrable and near-integrable (*non-ergodic*) regimes instead, we found that the heat transport is ballistic $J \propto L^0$.

Let us describe the numerical simulations. Again we consider the autonomous model (7) at three particular cases: (i) *quantum chaotic case* $H = H'(-2, 2, 3.375)$ at which LSD agrees with RMT and thus corresponds to the regime of quantum chaos, (ii) *integrable case* $H = H'(-2, 0, 3.375)$, at which LSD is close to the Poisson distribution, and (iii) *intermediate case* $H = H'(-2, 2, 7.875)$ at which the distribution LSD shows an intermediate character of weak level repulsion and exponential tail [59].

Let us now turn to study the energy transport in this model system. To this end, we need to couple both ends of the chain of spins to thermal baths at temperatures T_r, T_l . We have devised a simple way to simulate this coupling, namely the state of the spin in contact with the bath is statistically determined by a Boltzmann distribution with parameter T . Our model for the baths is analogous to the stochastic thermal baths used in classical simulations [64] and we thus call it a *quantum stochastic thermal bath*. In the representation basis of σ_n^z the wavefunction at time t can be written as

$$|\psi(t)\rangle = \sum_{s_0, s_1, \dots, s_{L-1}} C_{s_0, s_1, \dots, s_{L-1}}(t) |s_0, s_1, \dots, s_{L-1}\rangle, \quad (19)$$

where $s_n = 0, 1$ represents the *up*, *down* state of the n th spin, respectively. The wavefunction at time t is obtained from the unitary evolution operator $U(t) = \exp(-iHt)$. The interaction with the bath is not included in the unitary evolution. Instead, we assume that the spin chain and the bath interact only at discrete times with period τ at which the states of the leftmost (s_0) and the rightmost (s_{L-1}) spins are stochastically reset. Thus, the evolution of the wavefunction from time t to time $t + \tau$ can be represented as

$$|\psi(t + \tau)\rangle = \Xi(\beta_l, \beta_r)U(\tau)|\psi(t)\rangle, \tag{20}$$

where $\Xi(\beta_l, \beta_r)$ represents the *stochastic* action of the interaction with the left and right baths at temperatures β_l^{-1} and β_r^{-1} respectively.

The action of $\Xi(\beta_l, \beta_r)$ takes place in several steps.

- (i) The wavefunction is first rotated by the angle $\alpha = \arctan(h_x/h_z)$ to the eigenbasis of the components $\sigma_l = \vec{h} \cdot \vec{\sigma}_0/h$, $\sigma_r = \vec{h} \cdot \vec{\sigma}_{L-1}/h$ of the edge spins along the field $\vec{h} = (h_x, 0, h_z)$, that is $|\psi\rangle \rightarrow e^{-i\alpha(\sigma_0^y + \sigma_{L-1}^y)/2}|\psi\rangle$. Here, $h = |\vec{h}|$ stands for the magnitude of the magnetic field.
- (ii) A local measurement of the observables σ_l, σ_r is performed. Then the state of the spins at the borders collapses to a state (s_0^*, s_{L-1}^*) with probability

$$p(s_0^*, s_{L-1}^*) = \sum_{s_1, \dots, s_{L-2}} |C_{s_0^*, s_1, \dots, s_{L-2}, s_{L-1}^*}|^2. \tag{21}$$

So, after choosing s_0^*, s_{L-1}^* , we put all coefficients $C_{s_0, s_1, \dots, s_{L-1}}$ with $(s_0, s_{L-1}) \neq (s_0^*, s_{L-1}^*)$ to zero.

- (iii) The new state of the edge spins (s_0, s_{L-1}) is stochastically chosen. After this action simulating the thermal interaction with the baths each of the edge spins is set to *down*, (*up*) state with probability $\mu, (1 - \mu)$. If the new state of s_0 , or s_{L-1} , is different than the one after step (ii), then a simple unitary spin flip is performed to the wavefunction. The probability $\mu(\beta)$ depends on the canonical temperature of each of the thermal baths:

$$\mu(\beta_j) = \frac{e^{\beta_j h}}{e^{-\beta_j h} + e^{\beta_j h}}; \quad j \in \{l, r\}. \tag{22}$$

- (iv) Finally, the wavefunction is rotated back to the σ_n^z basis, $|\psi\rangle \rightarrow e^{i\alpha(\sigma_0^y + \sigma_{L-1}^y)/2}|\psi\rangle$.

This completes the description of the interaction with the quantum stochastic bath. This interaction thus (periodically) resets the value of the local energy $h\sigma_{l,r}$ of the spins in contact with the baths. Therefore, the value of τ controls the strength of the coupling to the bath. We have found that, in our units, $\tau = 1$ provides an optimal choice. We have nevertheless performed simulations for other values of τ with qualitatively similar results. In particular, for weak couplings ($\tau \gtrsim 1$) the heat conductivity does not depend on the coupling strength.

Note that our method does not correspond to a standard stochastic unravelling of a master equation for the density operator (e.g., in the Lindblad form) [65]. However, we have tested that, using our prescription, averages over the ensemble of quantum trajectories or time averages of one given quantum trajectory are sufficient to reconstruct a density-matrix operator $\rho = |\psi(t)\rangle\langle\psi(t)|$ that correctly describes the internal thermal state of the system in and out of equilibrium. For each run the initial wavefunction $|\psi(0)\rangle$ of the system is chosen at random. The system is then evolved for some relaxation time τ_{rel} after which it is assumed to fluctuate around a unique steady state. Measurements are then performed as time averages of the expectation values of suitable observables. We further average these quantities over different random realizations of ‘quantum trajectories’. In order to compute the energy profile we write the Hamiltonian (7) in terms of local energy density operators H_n :

$$H_n = J\sigma_n^x\sigma_{n+1}^x + \frac{\vec{h}}{2} \cdot (\vec{\sigma}_n + \vec{\sigma}_{n+1}), \tag{23}$$

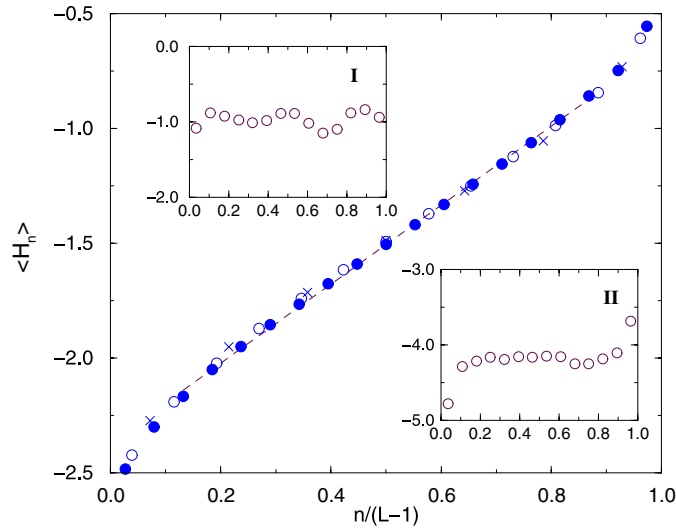


Figure 8. Out of equilibrium energy profile $\langle H_n \rangle$ for the chaotic chain. The temperatures of the baths $T_l = 5$ and $T_r = 50$ are both in the high temperature regime. Results for chains of size $L = 8$ (crosses), $L = 14$ (open circles) and $L = 20$ (solid circles) are shown. The dashed line was obtained from a linear fit of the data for $L = 20$ for the $L - 4$ central spins. Insets (I) and (II) show the energy profile for the integrable and intermediate cases, respectively, for $L = 15$.

such that the total Hamiltonian (7) can be written as $H = \sum_n H_n$ apart from the boundary corrections.

First we have performed equilibrium simulations in order to show that time-averaged expectation values of the local energy density can be used to determine canonical local temperature. To this end we set the left and right baths to the same temperature T . For low T , the energy per site $E = (1/L)\langle H \rangle$ saturates to a constant which, together with the entire energy profile $\langle H_n \rangle$, is determined by the ground state. However, for larger $T > 1$, the energy profile is constant within numerical accuracy, and numerical simulations give $E \sim -1/T$; all results being almost independent of L for $L \geq 6$. The numerical data for $E(T)$ can be well approximated with a simple calculation of energy density for a two-spin chain ($L = 2$) in a canonical state at temperature T , namely $E_{\text{can}}(T) = \text{tr} H_0 e^{-H_0/T} / \text{tr} e^{-H_0/T}$. Therefore, if the temperatures of both baths are in high T regime, then we can define the local temperature via the relation $T \propto -1/E$. We stress that equilibrium numerical data shown are *insensitive* to the nature of dynamics (consistent with results of [66]) whether being chaotic, regular or intermediate.

In figure 8, we show the energy profile $\langle H_n \rangle$ for an out of equilibrium simulation of the chaotic chain. In all non-equilibrium simulations, the temperatures of the baths were set to $T_l = 5$ and $T_r = 50$. After an appropriate scaling the profiles for different sizes L collapse to the same curve. More interesting, in the bulk of the chain the energy profile is in very good approximation linear. In contrast, we show that in the case of the integrable (inset I) and intermediate (inset II) chains, no energy gradient is created which is a characteristic of ballistic transport.

We now define the local current operators through the equation of continuity: $\partial_t H_n = i[H, H_n] = -(J_{n+1} - J_n)$, requiring that $J_n = -i[H_n, H_{n-1}]$. Using equations (23) and (7) the local heat current operators are explicitly given by $J_n = h_z J (\sigma_{n-1}^x - \sigma_{n+1}^x) \sigma_n^y$. In figure 9, we plot $J/\Delta E$ as a function of the size L of the system for sizes up to $L = 20$. The mean

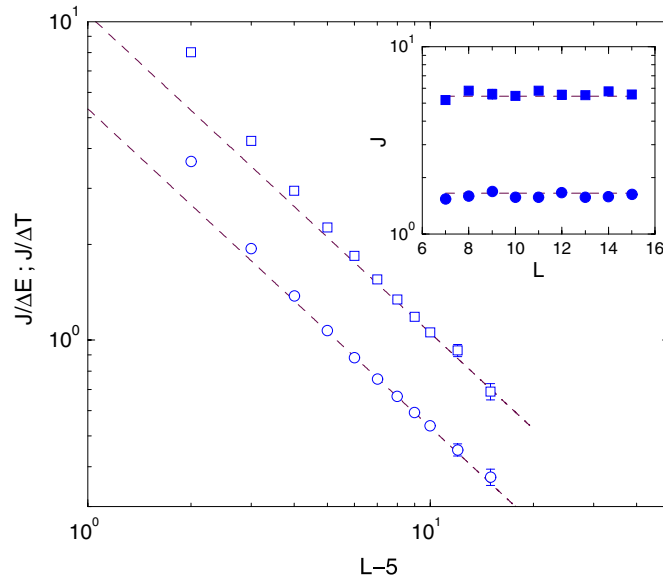


Figure 9. Size dependence of the energy current in the chaotic chain with $T_l = 5$ and $T_r = 50$. We show $J/\Delta E$ (open circles) and $J/\Delta T$ (open squares). The dashed lines correspond to $1/\Delta L$ scaling. In the inset, the size dependence of the energy current is shown for the integrable (solid circles) and the intermediate (solid squares) cases.

current J is calculated as an average of $\langle J_n \rangle$ over time and space n . The energy difference was obtained from the energy profile as $\Delta E = \langle H_{L-3} \rangle - \langle H_2 \rangle$. Two spins near each bath have been discarded in order to be in the bulk regime. Since $\Delta L = L - 5$ is an effective size of the truncated system, the observed $1/\Delta L$ dependence confirms that the transport is normal (diffusive). Moreover, also the quantity $J/\Delta T$, where $\Delta T = -1/\langle H_{L-3} \rangle + 1/\langle H_2 \rangle$, shows the correct scaling with the size L . On the other hand, in integrable and intermediate chains we have observed that the average heat current does not depend on the size $J \propto L^0$, clearly indicating the ballistic transport.

7. Quantum relaxation and complexity in a toy model: kicked Ising chain

Let us now come back to the kicked Ising model (1) and try to consider some very elementary but fundamental questions considering its dynamics and non-equilibrium statistical mechanics. Observing data of figure 1 in section 4 one can conclude that the model perhaps displays an interesting order to chaos, or non-ergodicity to ergodicity transition when the integrability breaking parameter is increased. Now we would like to inspect this transition more closely, and in particular understand the rate of relaxation to equilibrium in the ergodic and mixing case. We should stress right from the start that we are unable to prove any non-trivial statements about the model, but we can provide many suggestive numerical experiments which can be performed in a rather efficient way. We have learned in section 5 that it may be more fruitful to consider time evolution in the operator algebra spaces instead of in the spaces of pure states. Let us go now a bit deeper into this subject.

For some related results on high-temperature relaxation in isolated conservative many-body quantum systems see e.g. [67–71].

7.1. Time automorphism

Time automorphism on unital quasi-local C^* algebra (see e.g. [72] for introduction into the subject) $\mathcal{A}_{\mathbb{Z}}$, $\mathbf{T} : \mathcal{A}_{\mathbb{Z}} \rightarrow \mathcal{A}_{\mathbb{Z}}$ of an infinite KI lattice, for one period of the kick, can be explicitly constructed by the following observations.

Formally, for any $A \in \mathcal{A}_{\mathbb{Z}}$, $\mathbf{T}A := U^\dagger A U$, where U is given by either (3), (4), (6). Let $\mathcal{A}_{[m,n]}$, with $m \leq n$, denote a finite, local (4^{n-m+1})-dimensional algebra on a sub-lattice $[m, n] \subset \mathbb{Z}$, which is spanned by operators $\sigma_m^{s_m} \sigma_{m+1}^{s_{m+1}} \cdots \sigma_n^{s_n}$. It is straightforward to prove that dynamics is *strictly local*

$$\mathbf{T} : \mathcal{A}_{[m,n]} \rightarrow \mathcal{A}_{[m-1,n+1]}. \quad (24)$$

In other words, the homomorphism \mathbf{T} (24) is a simple nontrivial example of a quantum cellular automaton as defined by Schumacher and Werner [56].

$\mathcal{A}_{\mathbb{Z}}$ can also be treated as a Hilbert space with respect to the following inner product $\langle A|B \rangle = \omega(A^\dagger B)$, where $\omega(A)$ is a tracial state, $\omega(A) = 2^{-(n-m+1)} \text{tr} A$ for $A \in \mathcal{A}_{[m,n]}$. This Hilbert space can be in fact considered as a 1D lattice of four-level quantum systems (qudits with $d = 4$) with the orthonormal basis $|\dots, s_{-1}, s_0, s_1, \dots\rangle \equiv \cdots \sigma_{-1}^{s_{-1}} \sigma_0^{s_0} \sigma_1^{s_1} \cdots$ labelled by an infinite sequence of base-4 digits $s_j \in \mathbb{Z}_4$. Restricting for a moment to a dimer lattice $\mathcal{A}_{[j,j+1]}$, we can write the adjoint action of a 2-qubit gate W in terms of a 16×16 unitary matrix

$$\mathbf{W}_{j,j+1} |s_j, s_{j+1}\rangle = W^\dagger \sigma_j^{s_j} \sigma_{j+1}^{s_{j+1}} W = \sum_{r_j, r_{j+1} \in \mathbb{Z}_4} |r_j, r_{j+1}\rangle \mathbf{W}_{(r_j, r_{j+1}), (s_j, s_{j+1})} \quad (25)$$

where, very explicitly

$$\mathbf{W}_{(r_1, r_2), (s_1, s_2)} = \frac{1}{4} \text{tr}[(\sigma^{r_1} \otimes \sigma^{r_2}) W^\dagger (\sigma^{s_1} \otimes \sigma^{s_2}) W]. \quad (26)$$

We should note that the map is unital $\mathbf{W}|0, 0\rangle = |0, 0\rangle$, and that due to anti-unitary symmetry of the KI model, the matrix \mathbf{W} is *real*. We extend the map $\mathbf{W}_{j,j+1}$ to entire algebra $\mathcal{A}_{\mathbb{Z}}$ by $\mathbf{W}_{j,j+1}(A \otimes B) = \mathbf{W}_{j,j+1}(A) \otimes B$, for any $A \in \mathcal{A}_{[j,j+1]}$, $B \in \mathcal{A}_{\mathbb{Z}-[j,j+1]}$.

Now, following protocol (6) we finish the construction of the time automorphism as a string of right-to-left ordered 2-qudit (with $d = 4$) gates

$$\mathbf{T} = \prod_{j \in \mathbb{Z}} \mathbf{W}_{j,j+1}. \quad (27)$$

Explicitly, for any local observable $A = \sum_{s_m, s_{m+1}, \dots, s_n} a_{(s_m, s_{m+1}, \dots, s_n)} |s_m, s_{m+1}, \dots, s_n\rangle \in \mathcal{A}_{[m,n]}$, we have the following.

Algorithm 1

- (i) Set an initial vector: $a_{(s_{m-1}, s_m, \dots, s_n, s_{n+1})}^{(0)} = \delta_{s_{m-1}, 0} a_{(s_m, \dots, s_n)} \delta_{s_{n+1}, 0}$.
(ii) For $k = 0, 1, \dots, n - m + 1$:

$$a_{(s_{m-1}, s_m, \dots, s_n, s_{n+1})}^{(k+1)} = \sum_{r, r' \in \mathbb{Z}_4} \mathbf{W}_{(s_{m-1+k}, s_{m+k}), (r, r')} a_{(s_{m-1}, \dots, s_{m+k-2}, r', s_{m+k+1}, \dots, s_{n+1})}^{(k)}. \quad (28)$$

- (iii) The result is $\mathbf{T}A = \sum_{s_{m-1}, s_m, \dots, s_n} a_{(s_{m-1}, s_m, \dots, s_{n+1})}^{(n-m+2)} |s_{m-1}, s_m, \dots, s_{n+1}\rangle$.

The algorithm produces exact result in $(n - m + 2)4^{n-m+4}$ multiplications and about the same number of additions. Let $\mathbf{P}_{[m,n]} : \mathcal{A}_{\mathbb{Z}} \rightarrow \mathcal{A}_{[m,n]}$ denote a *linear orthogonal projector*, satisfying $\mathbf{P}_{[m,n]}(A \otimes E) = (\mathbb{1}|E)A$ if $A \in \mathcal{A}_{[m,n]}$, $E \in \mathcal{A}_{\mathbb{Z}-[m,n]}$. Let us define a truncated time-evolution operator $\mathbf{T}_{[m,n]} = \mathbf{P}_{[m,n]} \mathbf{T} : \mathcal{A}_{[m,n]} \rightarrow \mathcal{A}_{[m,n]}$ which we can actually implement on a computer with a finite memory register.

The ‘infinite-temperature’ time correlation function of (traceless) local quantum observables $A, B \in \mathcal{A}_{[m,n]}$ can be written as $C_{BA}(t) = (B|\mathbf{T}^t A)$, where $t \in \mathbb{Z}$. An interesting question is, up to what time t the $C_{BA}(t)$ can be computed numerically exactly with a finite computer register $[m-l, n+l]$ of $r = n - m + 1 + 2l$ qudits of size 4^r ? Due to the locality (24) of time homomorphism one can easily prove that

$$(B|\mathbf{T}^t A) = (B|\mathbf{T}_{[m-l,n+l]}^t A), \quad \text{for } t \leq 2l, \tag{29}$$

hence the correlation functions are computable exactly up to time $2l$, and as we shall see later, the truncated correlation function $C_{BA}^{(r)}(t) = (B|\mathbf{T}_{[m-r,n+r]}^t A)$ often well approximates $C_{BA}(t)$ even at later times, or even its asymptotic decay.

Let us continue our discussion by considering time evolution for *translationally invariant extensive* (TIE) observables. Given some quasi-local observable $A \in \mathcal{A}_{\mathbb{Z}}$ we shall construct the corresponding TIE observable by a formal mapping, $A \rightarrow \mathbf{F}(A) = \sum_{x \in \mathbb{Z}} \mathbf{S}_x(A)$ in terms of lattice translation automorphisms $\mathbf{S}_x : \mathcal{A}_{\mathbb{Z}} \rightarrow \mathcal{A}_{\mathbb{Z}}, \mathbf{S}_x(\sigma_j^s) = \sigma_{j+x}^s$. The image of the entire quasi-local algebra under this mapping, $\mathcal{Z} = \mathbf{F}(\mathcal{A}_{\mathbb{Z}})$, is not a C^* algebra, but it is a linear space which can be again turned into a Hilbert space with the following inner product:

$$((X|Y)) = \lim_{n \rightarrow \infty} \frac{1}{2n+1} (\mathbf{P}_{[-n,n]}(X)|\mathbf{P}_{[-n,n]}(Y)), \tag{30}$$

where the domain of projector $\mathbf{P}_{[-n,n]}$ is extended to \mathcal{Z} by continuity. The orthonormal basis of \mathcal{Z} is given by TIE observables $Z_{(c_0,c_1,\dots,c_{r-1})} = \mathbf{F}(\sigma_0^{c_0} \sigma_1^{c_1} \dots \sigma_{r-1}^{c_{r-1}})$, for orders $r = 1, 2, \dots$, and for uniqueness of notation, requiring $c_0, c_{r-1} \neq 0$. We shall interchangeably represent finite sequences of base-4 digits with integers, $(c_0, c_1, \dots, c_{r-1}) \equiv c = \sum_{j=0}^{r-1} c_j 4^j$. Let \mathcal{Z}_r be $(3 \times 4^{r-1})$ -dimensional subspace spanned by TIE observables Z_c with order $\leq r$, i.e. for c having at most r base-4 digits, so we have an inclusion sequence $\mathcal{Z}_1 \subset \mathcal{Z}_2, \dots, \subset \mathcal{Z}$.

Since time and space automorphisms commute $\mathbf{TS}_x = \mathbf{S}_x \mathbf{T}$, one can immediately extend the time map onto the space of TIE observables, $\hat{\mathbf{T}} : \mathcal{Z} \rightarrow \mathcal{Z}$ by continuity. Formally, we have $\hat{\mathbf{T}}\mathbf{F} = \mathbf{F}\mathbf{T}$. Furthermore, locality (24) implies

$$\hat{\mathbf{T}} : \mathcal{Z}_r \rightarrow \mathcal{Z}_{r+2}, \tag{31}$$

so we can write a simple adaptation of algorithm 1 for explicit construction of a time map of an arbitrary finite-order TIE observable $Y = \sum_{0 < c < 4^r}^{c \neq 0 \pmod{4}} y_c Z_c \in \mathcal{Z}_r$.

Algorithm 2

- (i) Take the following pre-image of the TIE observable $A = \sum_{0 < c < 4^r}^{c \neq 0 \pmod{4}} y_c |4c) \in \mathcal{A}_{[1,r]}$, namely $\mathbf{F}(A) = Y$.
- (ii) Compute a_c of $\mathbf{T}(A) = \sum_{0 \leq c < 4^{r+2}} a_c |c) \in \mathcal{A}_{[0,r+1]}$ according to algorithm 1.
- (iii) Transforming back to \mathcal{Z} , the result reads

$$\hat{\mathbf{T}}(Y) = \mathbf{F}(\mathbf{T}(A)) = \sum_{0 < c < 4^{r+2}}^{c \neq 0 \pmod{4}} y'_c Z_c, \quad y'_c = \begin{cases} a_c + a_{4c} + a_{16c}, & c < 4^r; \\ a_c + a_{4c}, & 4^r \leq c < 4^{r+1}; \\ a_c, & c \geq 4^{r+1}. \end{cases} \tag{32}$$

Let us further define the *natural truncations* of TIE space to order $r, \hat{\mathbf{P}}_r : \mathcal{Z} \rightarrow \mathcal{Z}$ as orthogonal projections $\hat{\mathbf{P}}_r(X) = \sum_{0 < c < 4^r}^{c \neq 0 \pmod{4}} Z_c((Z_c|X))$, and truncated time-evolution operators $\hat{\mathbf{T}}_r = \hat{\mathbf{P}}_r \hat{\mathbf{T}} : \mathcal{Z}_r \rightarrow \mathcal{Z}_r$, which are naturally implemented on a computer by simply truncating overflowing coefficients y'_c .

Physically interesting question now concerns computation of time correlation functions between a pair of finite-order (say q) TIE observables $X, Y \in \mathcal{Z}_q$, namely $C_{YX}(t) = ((Y|\hat{\mathbf{T}}^t X))$; for example in figure 1 we have shown the case of $X = Y = Z_3$. As a

consequence of locality (24) and translational invariance, we find that the truncated evolution on \mathcal{Z}_r reproduces correlation functions exactly

$$((B|\hat{\mathbf{T}}^t A)) = ((B|\hat{\mathbf{T}}_r^t A)), \quad \text{for } t \leq r - q. \quad (33)$$

Few remarks are in order. (i) Truncated translationally invariant time evolution $\hat{\mathbf{T}}_r$ is perhaps more natural object to study than truncated local time evolution $\mathbf{T}_{[m,n]}$, for a simple reason that the truncation $\hat{\mathbf{P}}_r$ commutes with a shift \mathbf{S}_x , while $\mathbf{P}_{[m,n]}$ does not. (ii) A space \mathcal{Z} can be identified with translationally invariant linear functionals over $\mathcal{A}_{\mathbb{Z}}$, namely $X(A) = ((X|\mathbf{F}A))$, $X \in \mathcal{Z}$, $A \in \mathcal{A}_{\mathbb{Z}}$. We have $(\hat{\mathbf{T}}^\dagger X)(A) = X(\mathbf{T}A)$ and $(\hat{\mathbf{T}}X)(A) = X(\mathbf{T}^\dagger A)$, where Hermitian adjoint maps $\hat{\mathbf{T}}^\dagger$ and \mathbf{T}^\dagger simply correspond to *time reversed* dynamics. (iii) Convex subspace of positive translationally invariant functionals $\mathcal{W} \subset \mathcal{Z}$ is an interesting invariant subspace of physical states, $\hat{\mathbf{T}}\mathcal{W} \subseteq \mathcal{W}$.

7.2. Relaxation and quantum Ruelle resonances

In classical mechanics of chaotic systems one typically observes that states (phase-space densities) develop small details in the course of time evolution at an exponential average rate. Consequently, introducing a small stochastic noise of strength ϵ to a Perron–Frobenius operator (PFO, i.e. Liouvillian propagator for discrete time dynamics) makes it non-unitary and shifts its spectrum inside the unit circle. Typically, the effect of noise is equivalent to an ultraviolet cutoff—truncation of a PFO—at the Fourier scale $k \sim 1/\epsilon$, and often the leading eigenvalues of the truncated PFO—the so-called Ruelle resonances—remain frozen inside the unit circle in the limit $\epsilon \rightarrow 0$ (or $k \rightarrow \infty$) [73]. For a general introduction to relaxation phenomena in classical Hamiltonian dynamics see e.g. [74].

Let us now draw some analogies with our quantum setting. We have seen that the evolution $\hat{\mathbf{T}}$ somehow most closely resembles Liouvillian evolution of classical Hamiltonian dynamics. In Hilbert space topology, the operator $\hat{\mathbf{T}}$ is unitary and its spectrum lies on a unit circle, just like in the case of a classical PFO. However, truncated $(3 \times 4^{r-1}) \times (3 \times 4^{r-1})$ matrices $\hat{\mathbf{T}}_r$ represent natural ‘ultraviolet’ cutoff truncations for increasing orders r . Let us check numerically if some eigenvalues of these matrices remain frozen when $r \rightarrow \infty$.

Indeed, as we demonstrate in figure 10, we find several eigenvalues which converge as r increases in the case of a strongly non-integrable (quantum chaotic) case, with a gap between an eigenvalue of maximal modulus and the unit circle, whereas in the integrable case a set of r eigenvalues touches the unit circle (actually eigenvalue 1 is r -fold degenerate). Numerical results suggest the following speculative conclusions. Let e^{-q_n} be the converged (frozen) eigenvalues of $\hat{\mathbf{T}}_r$, and $\{\Theta_n^R\}$, $\{\Theta_n^L\}$ the corresponding *right* and *left* eigenvectors, respectively. Then for an arbitrary pair $X, Y \in \mathcal{Z}$, the time correlation function can be expressed in terms of spectral decomposition (see e.g. [74])

$$C_{YX}(t) \sim \sum_n w_n e^{-q_n t}, \quad w_n = \frac{((Y|\Theta_n^R))((\Theta_n^L|X))}{((\Theta_n^L|\Theta_n^R))}. \quad (34)$$

The above relation is the contribution of the point spectrum and is exact if the spectrum is pure point. However, in classical cases, one may quite typically have various singular components and branch cuts [74]. Note that the denominator $((\Theta_n^L|\Theta_n^R))$ is finite, although both vectors should have infinite l^2 norm $((\Theta_n^L|\Theta_n^L)) = \infty$, $((\Theta_n^R|\Theta_n^R)) = \infty$, for any eigenvalue away from the unit circle, $\text{Re } q_n \neq 0$.

There is a simple relation between the spectrum of the PFO and the ergodic properties of dynamics.

- (i) If there is a *spectral gap*, i.e. there exists $\lambda > 0$ such that for all n , $|e^{-q_n}| \leq \exp(-\lambda) < 1$, then dynamics is *exponentially mixing*, $C_{YX}(t) \leq C \exp(-\lambda t)$.

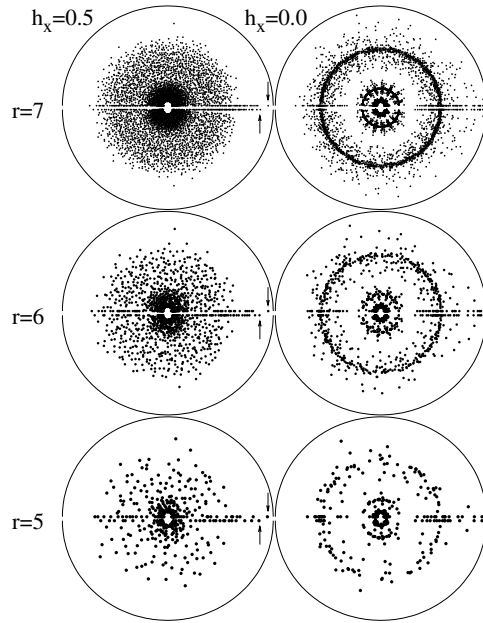


Figure 10. The spectra of truncated transfer operators $\hat{\mathbf{T}}_r$, for $r = 5, 6, 7$, in strongly non-integrable case $J = 0.7, h_x = 0.5, h_z = 1.1$ (left) and integrable case $J = 0.7, h_x = 0.0, h_z = 1.1$ (right), lying inside a complex unit circle (thin arcs). The points in upper/lower unit semi-discs correspond to positive/negative parity $\hat{\mathbf{R}}Z_{(c_0, c_1, \dots, c_{l-1})} = Z_{(c_{l-1}, \dots, c_1, c_0)}$ eigenvectors. Arrows point at converged positions of the leading eigenvalue e^{-q_1} .

- (ii) If some eigenvalues are on the unit circle, meaning that the corresponding eigenvector coefficients should be in l^2 , then the system is *non-mixing* since there are correlation functions which do not decay.
- (iii) If some eigenvalues are at 1 then the system is *non-ergodic* since the correlation functions may have non-vanishing time averages. If Q_n is a complete set of orthonormalized eigenvectors corresponding to eigenvalue 1, $((Q_n | Q_m)) = \delta_{n,m}$ (and note that since we are on the unit circle: $Q_n^R = Q_n^L$) then

$$D_X := \overline{C_{XX}(t)} = \sum_n |((X | Q_n))|^2. \tag{35}$$

Latter (iii) happens in generic completely integrable quantum lattices, where Q_n correspond to an infinite sequence of conservation laws [75]. Furthermore, we have a strong numerical evidence that also in certain non-integrable quantum lattices [76], and also in the KI model [17], one has a regime where few normalizable (‘pseudo-local’) but not local (like in integrable models) conservation laws exist. This situation we call the regime of *intermediate* dynamics and is characterized by a non-vanishing *stiffness* $D_X \neq 0$ signalling *ballistic transport*.

In figure 11, we compare the time autocorrelation function of the transverse magnetization, $M = \sum_{j \in \mathbb{Z}} \sigma_j^z = Z_3$, computed in three different ways: (1) from exact time evolution $C_L(t) = \frac{1}{L} \langle M U_L^{-t} M U_L^t \rangle$ on a finite lattice of length L with periodic boundary conditions, (2) iteration of truncated TA matrix on infinite lattice $C_r(t) = ((M | \hat{\mathbf{T}}_r^t M))$, and (3) asymptotics based on (few) leading eigenvalue resonance(s) (using formula (34) in terms of q_n and w_n).

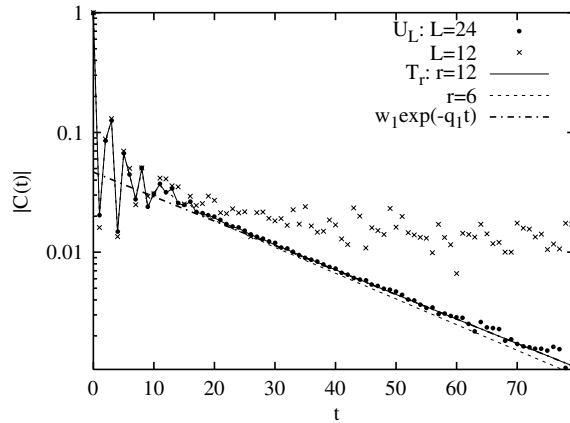


Figure 11. Correlation function of the transverse magnetization $C(t) = \langle (M|M(t)) \rangle$, in the mixing case $J = 0.7, h_x = 0.5, h_z = 1.1$, computed from finite system dynamics for different sizes L (symbols), and from truncated adjoint propagators \hat{T}_r of infinite systems (curves) for different truncation orders r . The chain line indicates the asymptotics based on the leading quantum Ruelle resonance.

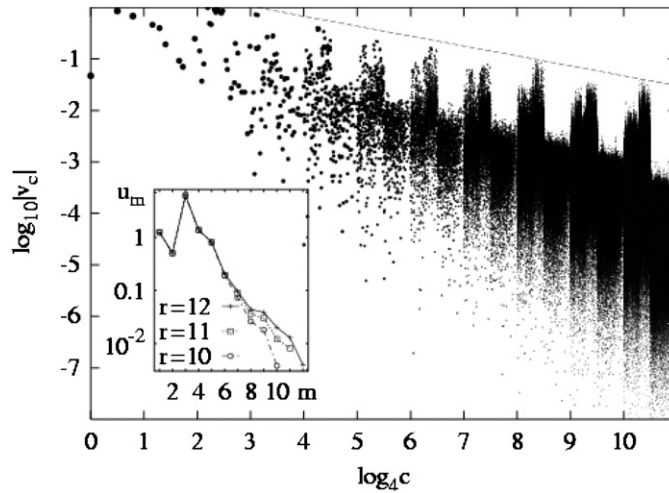


Figure 12. Eigenvector $\Theta_1^R = \sum_c v_c Z_c$, of the leading eigenvalue (closest to a unit circle) has statistically self-similar structure, when expanded in Z_c . We plot the modulus of coefficients v_c (in the log scale) of the right eigenvector versus the log (in base 4) of the integer code c . Dashed line indicates power-law scaling $c^{-\nu}$ with slope $\nu = 0.32$. In the inset, we plot partial scalar products $u_m = \sum_{c \neq 0 \pmod{4}}^{c < 4^m - 1} ((\Theta_1^L | Z_c)) ((Z_c | \Theta_1^R))$ with the corresponding left eigenvector within fixed orders m .

We note that the leading eigenvalue and eigenvector of truncated TA \hat{T}_r can most efficiently be computed using our algorithm 2 as a key step of an iterative *power method*. In this way, we were able to perform calculations of the leading Ruelle resonances up to $r = 15$ in contrast to full diagonalization of truncated matrices \hat{T}_r which were feasible only up to $r = 7$. Let us observe the structure of the eigenvector coefficients $v_c^{L,R} = \langle (Z_c | \Theta_n^{L,R}) \rangle$ corresponding to the leading eigenvalue. Numerical results (see figure 12, see also subsection 7.5 later) strongly

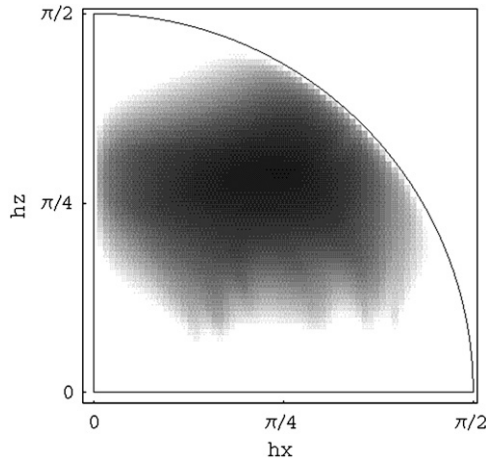


Figure 13. Two-dimensional numerical phase diagram for the kicked Ising lattice at cutoff order $r = 7$. The grey level indicates the spectral gap $\log \Delta$ of $\hat{\mathbf{T}}_r$ as a function of h_x and h_z at fixed $J = 0.7$. White regions correspond to $\Delta < 10^{-6}$.

suggest self-similar behaviour upon multiplying the code c by 4 which is a consequence of the fractal structure of the transfer matrix (see illustration in [77, 18]).

The stiffness D_X and the spectral gap $\Delta = |1 - e^{-q_1}|$ may be considered as *order parameters*, characterizing a particular kind of dynamical phase transition, namely the transition from non-ergodic dynamics—ordered phase, where $D_X \neq 0$ for a typical² X , or $\Delta = 0$, to an ergodic and mixing dynamics—disordered phase, where $D_X = 0$, for all traceless $X \in \mathcal{Z}$, or $\Delta > 0$. We know that the KI model is non-ergodic in integrable regimes. Let us consider a fixed transverse field case $h_x = 0$, and start to switch on a small amount of longitudinal field h_x . The interesting question is whether the transition happens for infinitesimal integrability breaking parameter h_x in TL, or at a finite *critical* field. In figure 13, we fix $J = 0.7$ and plot a two-dimensional phase diagram of the spectral gap $\Delta(h_x, h_z)$. It is clear that we have different behaviour in different regions of parameter space; for example we identify two transitions.

- (i) *Type I transition.* If the transverse field is roughly on the interval $h_z \in [0.7, 1.2]$, then the spectral gap opens in the fastest possible manner which is allowed by a $h_x \rightarrow -h_x$ symmetry and the analyticity of the problem, namely $\Delta \propto h_x^2$. See figure 14.
- (ii) *Type II transition.* If the initial transverse field $h_z < 0.7$, or $h_z > 1.2$, then the gap opens up in a much more abrupt—perhaps a discontinuous way. We give an example by scanning the diagonal transition, i.e. putting $h_x = h_z$ and increasing h_x from zero. Numerical results, shown in figure 15 cannot be made fully conclusive, but they are not inconsistent with a conclusion that an abrupt transition to ergodic behaviour takes place at $h_x = h_z \approx 0.3$.

7.3. Translationally invariant conservation laws as matrix product operators

There is another possibly interesting way of characterizing the transition, i.e. in terms of pseudo-local translationally invariant conservation laws [76]. Such conservation laws are the square normalizable elements $Q \in \mathcal{Z}$, which are mapped onto themselves under the dynamics

² Any observable X which is not orthogonal to all conservation laws Q_n , i.e. normalizable eigenvectors of $\hat{\mathbf{T}}$ with eigenvalue 1.

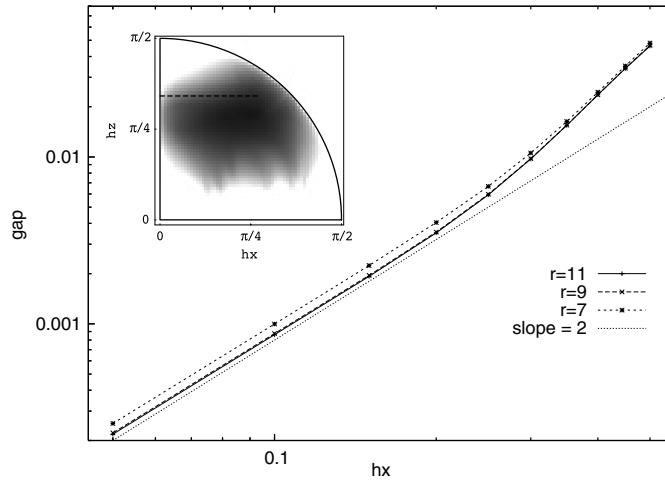


Figure 14. Type I transition. Spectral gap of \hat{T}_r as a function of h_x at $J = 0.7, h_z = 1.1$ at different truncation orders r . In the inset, we indicate a line of transition in a 2D phase diagram.

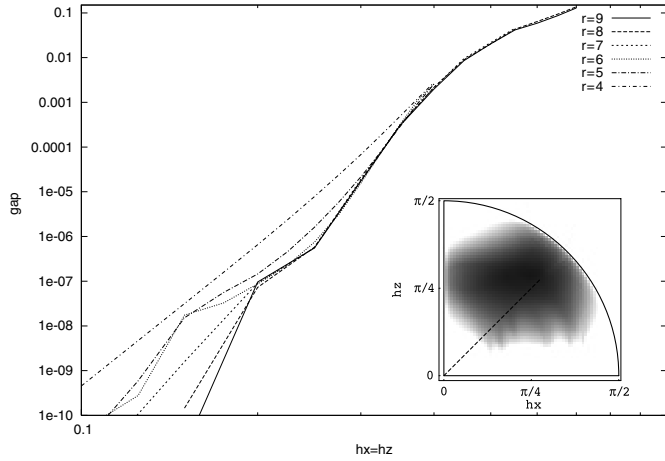


Figure 15. Type II transition. Spectral gap of \hat{T}_r as a function of $h_x = h_z$ at $J = 0.7$ at different truncation orders r . In the inset, we indicate a line of transition in a 2D phase diagram.

$\hat{T}(Q) = Q$. We shall first make a non-trivial variational MPO ansatz for elements of \mathcal{Z} , namely let us take an auxiliary vector space $\mathbb{C}^D = \mathbb{C}^{D_1} \oplus \mathbb{C}^{D_2} \oplus \mathbb{C}^{D_3}$, where $D = D_1 + D_2 + D_3$. Then any operator Q , which is formally written in terms of the MPO on the *infinite* spin chain

$$Q = \sum_{\dots s_{-1} s_0 s_1 \dots \in \mathbb{Z}_4} (\vec{a}_L \cdots A^{s_{-1}} A^{s_0} A^{s_1} \cdots \vec{a}_R) \cdots \sigma_{-1}^{s_{-1}} \sigma_0^{s_0} \sigma_1^{s_1} \cdots, \quad (36)$$

where $A^s \in \mathbb{C}^{D \times D}$, $\vec{a}_L, \vec{a}_R \in \mathbb{C}^D$ have the block matrix form (for $k = 1, 2, 3$):

$$A^0 = \begin{pmatrix} 1 & 0 & 0 \\ 0 & 1 & 0 \\ 0 & 0 & E_0 \end{pmatrix}, \quad A^k = \begin{pmatrix} 0 & * & * \\ 0 & 0 & 0 \\ 0 & * & E_k \end{pmatrix}, \quad \vec{a}_L = \begin{pmatrix} * \\ 0 \\ 0 \end{pmatrix}, \quad \vec{a}_R = \begin{pmatrix} 0 \\ * \\ 0 \end{pmatrix}, \quad (37)$$

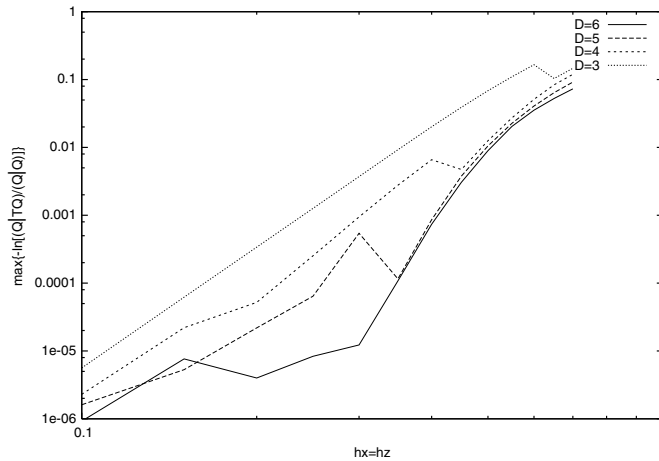


Figure 16. Optimized fidelity (38)—in the log scale—for approximate conservation laws within MPO spaces of different fixed dimensions D (indicated in the legend) for an infinite KI lattice along the diagonal type II transition with $h_x = h_z$ and $J = 0.7$. A simple stochastic search has been used to maximize fidelity $F(Q)$. Note the similarity with the gap curve shown in figure 15.

represents a translationally invariant pseudo-local operator, i.e. an element of \mathcal{Z} , provided that $\|E_0\| < 1$ and $\|E_1\|^2 + \|E_2\|^2 + \|E_3\|^3 < 1$, where $\|\cdot\|$ is a spectral matrix norm and $*$'s stand for arbitrary matrices/vectors. Of course, converse cannot be generally true, not any element of \mathcal{Z} can be written as an MPO (36) with finite D , but still there are elements of the form (36), (37) which are not in \mathcal{Z}_r for any finite r .

There exists a straightforward algorithm which performs time evolution on the MPO data (37), namely $\hat{\mathbf{T}}(Q)$ is also of the form (36), (37) with dimension $D' \leq 2D$. We shall now make the following simple numerical experiment. Let us fix D , setting $D_1 = D_2 = 1$ representing the simplest $\hat{\mathbf{T}}$ -invariant subclass of (36), (37), and optimize (maximize) the fidelity-like quantity

$$F(Q) = \frac{|((Q|\hat{\mathbf{T}}Q))|}{((Q|Q))}, \tag{38}$$

within this class of operators. Let us write an operator which maximizes $F(Q)$ for a given D as Q_D . Note that $1 - F(Q_D)$ gives a strong-topology measure of conservation of observable Q_D in one step of time evolution, so $F(Q_D) = 1$ only for exact conservation laws. Increasing D may improve fidelity, if pseudo-local conservation laws exist to which Q_D may converge; however, in ergodic and mixing situation where no exact pseudo-local conservation laws exist, increasing D should have no significant effect to fidelity $F(Q_D)$. This is exactly what we observe in the KI model following a line of type II transition (see figure 16).

7.4. Operator-space entanglement measures and complexity of time evolution

Numerical results of section 5 suggested that operator-space entanglement measures can be used to characterize the complexity of time evolution, namely the minimal required rank D_ϵ of MPO ansatz is simply related to an entanglement entropy of a time-evolving local observable, which is interpreted as a Hilbert space vector. In order to make things as simple and precise as possible we go back to the time-evolution automorphism \mathbf{T} over the quasi-local spin algebra $\mathcal{A}_{\mathbb{Z}}$. Let us take some truncation order $r = 2n + 1$ and consider the

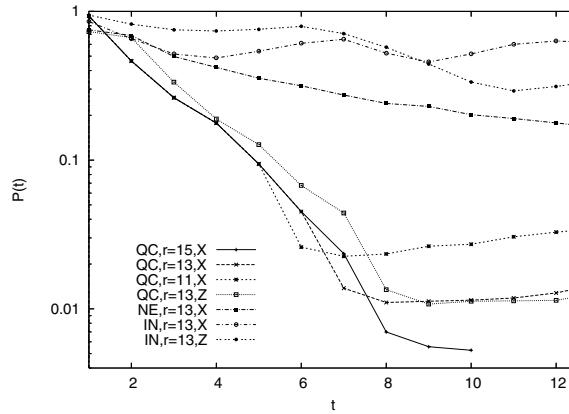


Figure 17. Purity $P^{(0,n)}(t)$ of reduced operator space density matrix for the KI lattice, with different cutoff sizes $r = 2n + 1 = 15, 13, 11$, and for two initial centred local operators $X = \sigma_0^x$ and $Z = \sigma_0^z$. Note exponential decay of purity for the QC case and saturation or slow decay of purity for the non-ergodic cases (IN, NE).

truncated map $\mathbf{T}_{[-n,n]}$. Starting with local operators on a single site $\mathcal{A}_{[0,0]}$ this truncated map is exact up to time $t = n$. Writing time-evolved observable at any instant of time as $A(t) = \mathbf{T}_{[-n,n]}^t A(0) = \sum_{\underline{s}} a_{(s_{-n}, \dots, s_n)}^{(t)} |s_{-n}, \dots, s_n\rangle$ in terms of a ‘wavefunction’ $a_{(s_{-n}, \dots, s_n)}^{(t)}$, and partitioning a sub-lattice at m , $-n < m \leq n$, as $[-n, n] = [-n, m-1] \cup [m, n]$, we can define a $(4^{n-m+1} \times 4^{n-m+1})$ -reduced super-density matrix as

$$R_{(s_m, \dots, s_n), (s'_m, \dots, s'_n)}^{(m,n)}(t) = \sum_{s_{-n}, \dots, s_{m-1}} a_{(s_{-n}, \dots, s_{m-1}, s_m, \dots, s_n)}^{(t)} a_{(s_{-n}, \dots, s_{m-1}, s'_m, \dots, s'_n)}^{(t)*}. \quad (39)$$

Since $A(t)$ is interpreted as a ‘pure state’, namely a vector from $\mathcal{A}_{[-n, m-1]} \otimes \mathcal{A}_{[m, n]}$, the operator-space entanglement is most simply characterized either by Von Neuman entropy $S^{(m,n)}(t) = -\text{tr} R^{(m,n)} \log R^{(m,n)}$, or linear entropy $S_2^{(m,n)}(t) = -\log P^{(m,n)}(t)$, where $P^{(m,n)}(t) = \text{tr}[R^{(m,n)}(t)]^2$ is a purity of reduced super-density matrix.

In figure 17, we plot the entanglement purity $P^{(0,n)}(t)$ —for close to symmetric bipartition $m = 0$ where the entanglement is expected to be maximal—for three different characteristic cases of the KI model, which will be in the following referred to as *quantum chaotic* (QC), $J = 0.7, h_x = 0.9, h_z = 0.9$, *integrable* (IN), $J = 0.7, h_x = 0, h_z = 0.9$, and *non-ergodic* (NE) non-integrable case, $J = 0.7, h_x = 0.2, h_z = 0.2$. We find that in the QC case purity decreases exponentially $P^{(0,n)}(t) = \exp(-h_q t)$, meaning $S_2(t) = h_q t$, where the exponent h_q is independent of the initial observable $A(0)$ and asymptotically independent of r . On the other hand, in the IN case $P^{(0,n)}(t)$ does not decay at all so the resulting dynamical entropy $h_q = 0$, whereas in the NE case $P^{(0,n)}(t)$ decays slowly, likely slower than exponentially.

7.5. Scaling invariance and the problem on semi-infinite lattice

The eigenvectors of $\hat{\mathbf{T}}$ corresponding to non-unimodular eigenvalues seem to exhibit a certain scaling invariance (figure 12). Here we would like to explore this property in a little bit more detail. For that purpose, we again explore the map $\mathbf{T}_{[-n,n]}$ on the quasi-local algebra $\mathcal{A}_{[-n,n]}$ since the representation of dynamics is conceptually simpler (algorithm 1) than dynamics $\hat{\mathbf{T}}_{2n+1}$ on \mathcal{Z}_{2n+1} . In particular, it is worth mentioning that if one traces out an additional qudit after

each time step, then the dynamics is exact on a *closed* set of $4^{n-m+1} \times 4^{n-m+1}$ super-density matrices and has a simple explicit form in terms of a completely positive matrix map³

$$R^{(m+1,n+1)}(t+1) = \text{tr}_0 \{ T_{n-m} [R^{(m,n)}(t) \otimes E_{00}] T_{n-m}^\dagger \}, \quad (40)$$

$$T_r = \prod_{0 \leq k \leq r} \mathbb{1}_4^{\otimes k} \otimes W \otimes \mathbb{1}_4^{\otimes (r-k)}, \quad (41)$$

namely no truncation is needed since at time $t+1$ we are describing an exact observable on $\mathcal{A}_{[-n-1,n+1]}$. We write $(\text{tr}_0 R)_{j,k} := \sum_{s=0}^3 R_{s+4j,s+4k}$ for tracing out the least significant qudit, and $E_{00} = |0\rangle\langle 0|$ is an elementary 4×4 projector. Note that T_{n-m} is just a matrix of $\mathbf{T}_{[m,n]}$ in the canonical basis $|s\rangle$. It is rather trivial to exactly solve this dynamics for a small finite $n-m$, however, this does not yield physically very useful information about the KI dynamics. One would wish to study the correct TL by first taking $n \rightarrow \infty$, and only after that $m, t \rightarrow \infty$; however, this task seems almost computationally intractable. Still, we were able to make some modest numerical experiments exploring this question, suggesting that for sufficiently strong integrability breaking (say the QC case) the asymptotic matrix $R^{(m,\infty)}(\infty)$ has a remarkable scale invariance if we coarse-grain it by tracing over its 4×4 blocks:

$$R^{(m+1,\infty)}(\infty) = \text{tr}_0 R^{(m,\infty)}(\infty) = \zeta R^{(m,\infty)}(\infty), \quad (42)$$

where ζ is some scaling factor. This seems to be true for both orders of the limits $t \rightarrow \infty, n \rightarrow \infty$, although better numerical results have been obtained for the ‘incorrect’ limit, namely letting the number of iterations $t \rightarrow \infty$ for a finite register size n , and then checking the convergence of results with increasing n .

Before discussing the numerical results we note another useful observation. Let us define and briefly study the KI chain on a *semi-infinite* lattice $\mathbb{Z}_+ = [0, \infty]$, with the Hamiltonian (1) for $L = \infty$ and open boundary condition on the left edge. Now we consider a quasi-local algebra $\mathcal{A}_{\mathbb{Z}_+}$. The time automorphism is again strictly local $\mathbf{T}^+ : \mathcal{A}_{[0,n]} \rightarrow \mathcal{A}_{[0,n+1]}$, and can be written as a semi-infinite product $\mathbf{T}^+ = \prod_{j \in \mathbb{Z}_+}^- \mathbf{W}_{j,j+1}$. In the definition of the truncated time map $\mathbf{T}_{[0,n]}^+ = \mathbf{P}_{[0,n]} \mathbf{T}^+ : \mathcal{A}_{[0,n]} \rightarrow \mathcal{A}_{[0,n]}$ truncation is needed only on the right edge. Note that due to this property, simulation of local observables (localized near the edge of the lattice) is twice as efficient than on the doubly infinite lattice, meaning that with the same size of computer register one can exactly simulate for twice longer times. For example, the computation of correlation functions $C_{BA}^+(t) := (B | [\mathbf{T}^+]^t A)$ is exact

$$(B | [\mathbf{T}^+]^t A) = (B | [\mathbf{T}_{[0,n]}^+]^t A), \quad \text{for } t \leq 2(n-q), \quad \text{if } A, B \in \mathcal{A}_{[0,q]}. \quad (43)$$

Numerically inspecting the correlation functions of a simple local spin $A = B = \sigma_0^x$ in figure 18, we find clear asymptotic exponential decay for the QC case, whereas for the IN and NE cases we find non-vanishing plateaus in the correlation function, i.e. non-vanishing stiffness $D^+ := \overline{C}^+ \neq 0$ which signals non-ergodicity and the existence of local (for integrable cases) and pseudo-local (for non-ergodic and non-integrable cases, e.g. NE) conservation laws of \mathbf{T}^+ . We note that the asymptotic correlation decay in non-integrable cases, say QC and NE, seems quite insensitive to increasing truncation order n —indicating that the leading eigenvalues of $\mathbf{T}_{[0,n]}^+$ remain frozen when increasing n . Note that the asymptotic exponents of correlation decay for a semi-infinite chain are not the same as for an infinite one, i.e. the point spectra of $\mathbf{T}_{[0,n]}^+$ and $\hat{\mathbf{T}}_n$ are in general different; however, we have some indications to believe that their phase diagrams should agree, namely ergodic regimes in the KI model on the semi-infinite chain model are in one-to-one correspondence with ergodic regimes of the model on an infinite chain.

³ When labelling tensor product matrix elements we shall always follow a convention that left factors are labelled with less significant digits, namely $(A \otimes B)_{j+j',d,k+k',d} = A_{j,k} B_{j',k'}$.

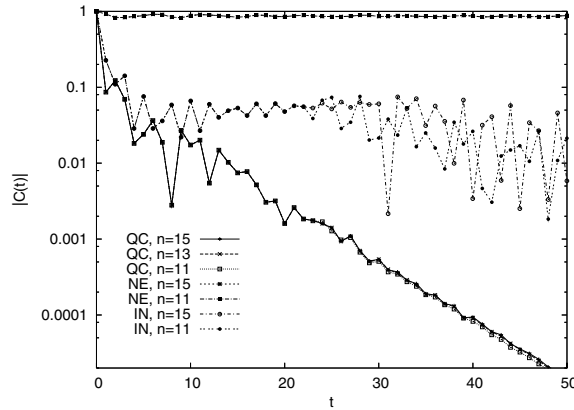


Figure 18. Decay of correlations $C^+(t) = \langle \sigma_0^x(t) \sigma_0^x \rangle$ for the semi-infinite KI lattice, with different cutoff sizes $n = 15, 13, 11$, and for different cases (QC, NE, IN), all indicated in the figure. Note that the two curves for the NE case are practically overlapping, and that all curves for different r 's are exactly overlapping until $t = 2r_{\text{smaller}}$.

However, the most remarkable feature of dynamics \mathbf{T}^+ is the following. Splitting the truncated semi-lattice as $[0, n] = [0, m-1] \cup [m, n]$ and following the time evolution of an observable $A(t) = [\mathbf{T}_{[0,n]}^+]^t A(0) = \sum_{\underline{s}} a_{(s_0, \dots, s_n)}^{(t)} |s_0, \dots, s_n\rangle$ in terms of a ‘super-wavefunction’ $a_{(s_0, \dots, s_n)}^{(t)}$, one can again define the reduced super-density matrix as

$$R_{(s_m, \dots, s_n), (s'_m, \dots, s'_n)}^{(m,n)}(t) = \sum_{s_0, \dots, s_{m-1}} a_{(s_0, \dots, s_{m-1}, s_m, \dots, s_n)}^{(t)} a_{(s_0, \dots, s_{m-1}, s'_m, \dots, s'_n)}^{(t)*}. \quad (44)$$

The dynamical equation for $R^{(m+1, n+1)}(t+1)$ in terms of $R^{(m,n)}(t)$ is *exactly the same* as for the doubly infinite lattice, namely equations (40), (41). Hence also the conjecture (42) on scaling invariance of $R^{(m,\infty)}(\infty)$ should be the same for the two lattice topologies. However, numerical computations are much easier and thus the results are more suggestive for the semi-infinite case.

Let us now discuss some numerical results. We have always started from a local initial operator $A(0) = \sigma_0^x$. We took n as large as allowed by existing computing resources, namely $n = 15$ for the semi-infinite chain and $n = 7$ for the infinite chain, and compared the data for asymptotic matrices $R^{(m,n)}(\infty)$ (in numerics t has been chosen such that the results converged, typically $t \approx 100$) with finite time data $R^{(m,n)}(t^*)$, where time t^* was set as large as allowed so that the data were still exact and no truncation was needed, typically $t^* \approx n$. In all cases, numerical results were quite insensitive to small changes in truncation order n . First, we have computed the scaling of the principal matrix element, or the *partial norms* $R_{00}^{(m,n)}(t) = \sum_{\dots, s_{m-2}, s_{m-1} \in \mathbb{Z}_4} |a_{(\dots, s_{m-2}, s_{m-1}, 0, 0, \dots)}^{(t)}|^2$ which, assuming (42), should asymptotically scale as $\propto \zeta^m$ (see figure 19). If asymptotic dynamics $t \rightarrow \infty$ is determined by normalizable eigenvectors of \mathbf{T}^+ , which necessarily correspond to uni-modular eigenvalues, then we should have $\zeta = 1$. In the QC case, a clear scaling was observed for both topologies (\mathbb{Z} and \mathbb{Z}^+) with the same exponent ζ , however, the exponent was slightly different for $R^{(m,n)}(\infty)$ and $R^{(m,n)}(t^*)$. In the cases of non-ergodic dynamics (NE and IN) the results for two topologies were quite different. For semi-infinite topology, we find very clearly that $\zeta = 1$ indicating that $A(t^*)$ and even $A(\infty)$ can be written as l^2 convergent sums of local operators.

As a more quantitative test of conjecture (42), we compare the upper-left (‘most important’) 16×16 block of the super-density matrix scaled to a unit principal element $R_{j,k}^p(t) \equiv R_{j,k}^{(m_0+p,n)}(t) / R_{0,0}^{(m_0+p,n)}(t)$. In figure 20, we plot the diagonal elements $R_{j,j}^p(t)$ for

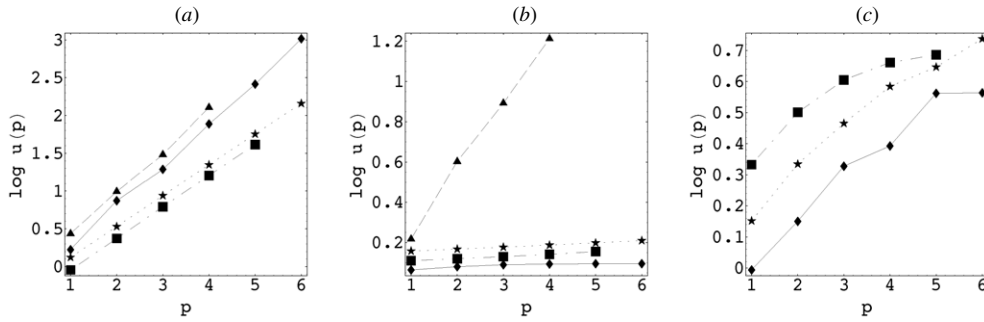


Figure 19. Scaling of the partial norms $u(p) = R_{0,0}^{(m_0+p,n)}(t)$ in the log scale (units are arbitrary) versus the partial tracing index p , for cases QC (a), NE (b) and IN (c). Diamonds, stars, and squares represent data for the semi-infinite KI lattice with truncation size $n = 15$, (diamonds, stars) and $n = 11$ (squares), all for $m_0 = 4$. Finite number of time steps $t = t^* = 17$ (diamonds), just before the absorbing boundary affects any of the data shown, is compared to steady state observable $t = \infty$ (stars). In the non-integrable cases (a), (b), data are compared also with the steady state $t = \infty$ simulation of the same local initial observable $A(0) = \sigma_0^x$ on the two-sided (doubly-infinite) KI lattice with truncation size $n = 7$ ($r = 15$), and $m_0 = 2$ (triangles).

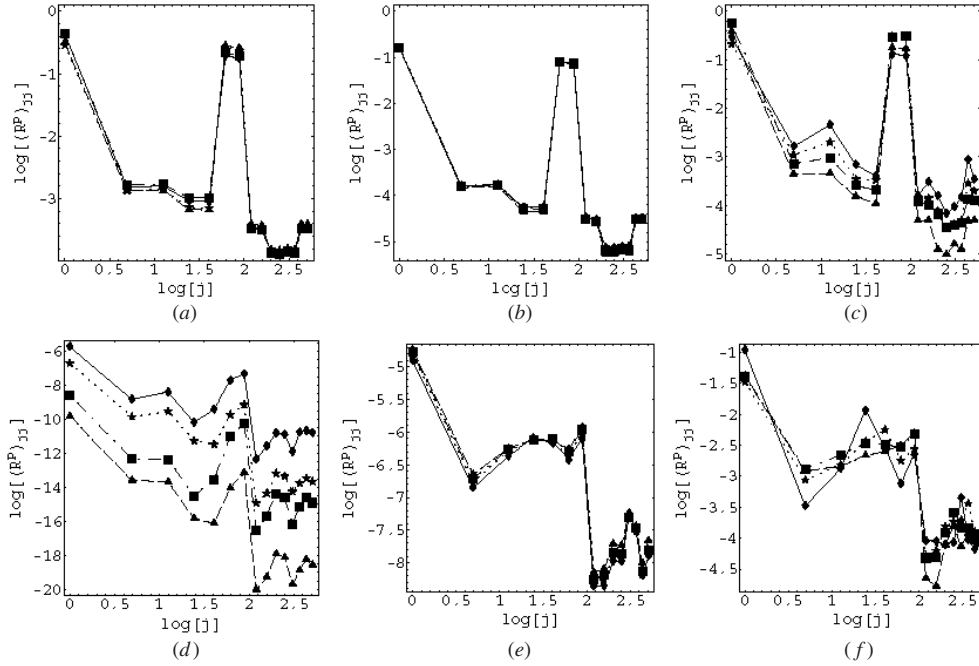


Figure 20. Scaling of the diagonal elements of scaled-reduced super-density matrices $R_{j,j}^p(t)$ for an initial tracing index $m_0 = 6$, and $p = 1$ (diamonds), $p = 2$ (stars), $p = 3$ (squares), $p = 4$ (triangles), for non-integrable cases of the KI chain on the semi-infinite lattice truncated at $n = 15$, namely for the case QC (a), (b), and the case NE (d), (e). Finite time data at $t = t^* = 17$ kicks are shown in (a), (d), while steady state observables $t = \infty$ are analysed in (b), (e), all starting from initial observable σ_0^x . For comparison, asymptotic steady state $t = \infty$ data for two-sided, doubly infinite KI chain, truncated at $r = 13$, and with initial tracing index $m_0 = 2$, are shown in (c), (f), namely for QC case (c) and NE case (f). Note that data in plot (b) are practically exactly overlapping.

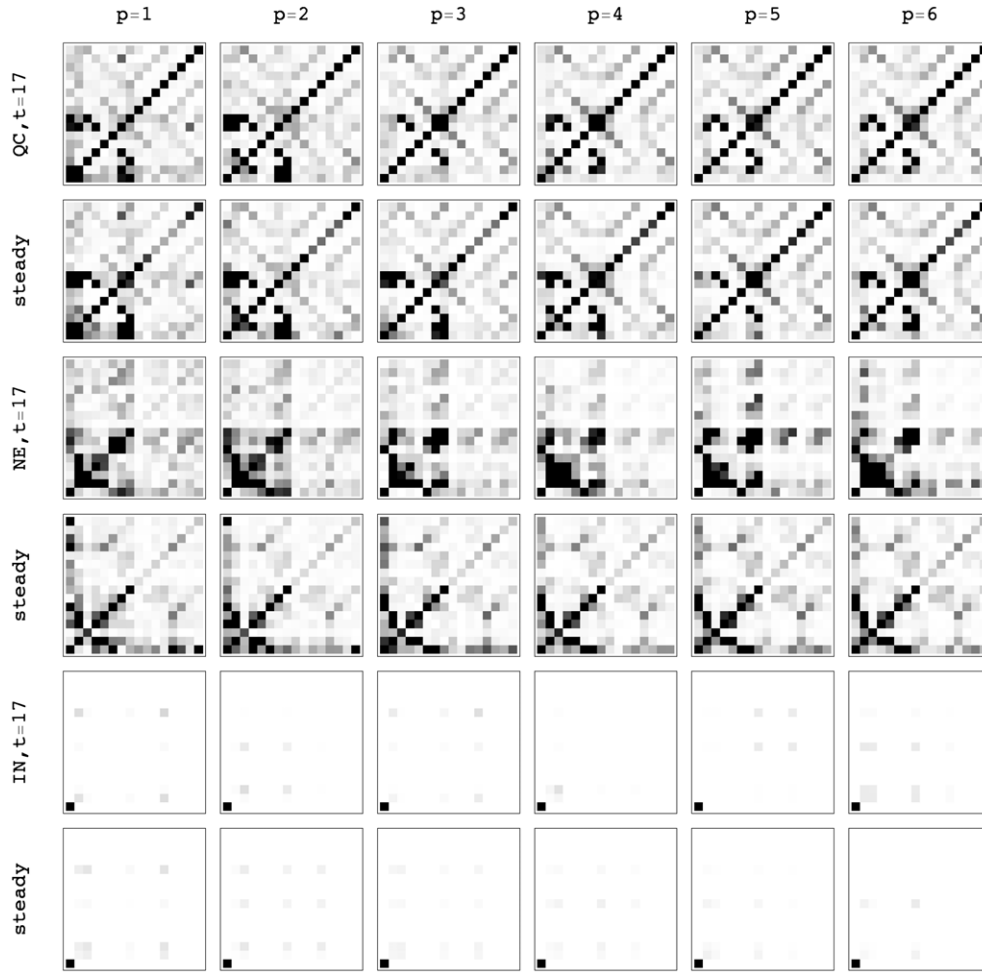


Figure 21. Scaling of scaled-reduced super-density matrices $R_{j,k}^p(t)$ —the grayness level is proportional to $|R_{j,k}^p(t)|$ —for the initial tracing index $m_0 = 4$, and $p = 1, \dots, 6$ (columns plots), for six different cases, QC, NE, and IN of the truncated semi-infinite KI lattice ($n = 15$), at finite time $t = t^* = 17$, and an asymptotic steady state $t = \infty$ (row plots), always starting from initial observable σ_0^x . 16×16 ‘most important’ matrix elements are plotted with the matrix site $j = k = 0$ at lower-left corner.

different p , while in figure 21 we plot 2D charts of the entire scaled density matrices $R_{j,k}^p(t)$. Indeed, we find for the QC case that the matrix $R_{j,k}^p(t)$ is practically insensitive to increasing truncation (p) and to topology of the lattice (semi-infinite versus infinite), both for finite time $t = t^*$ and ‘steady-state’ $t = \infty$. On the other hand, in non-ergodic cases, the scaling (42) is typically broken. However, it seems to be observed in the steady state ($t = t^*$) of the NE case, which is (in our setting) probably a non-physical but still quite robust effect due to truncation (a kind of absorbing boundary condition).

Summarizing this subsection, we conjectured that in the regime of quantum chaos reduced super-density matrices of time-evolved observables typically obey the scaling law (42) with the exponent ζ which only depends on global dynamics on quasi-local algebra of observables and not on a particular choice of initial observable. We expect that accurate numerical calculations

of exponent ζ would be possible within a certain quantum dynamic renormalization group scheme, however its precise formulation at present remains an open problem.

7.6. Dynamical entropies

In section 5, further elaborated in subsection 7.4, we have proposed an entanglement in operator space of quasi-local algebra as a possible new measure of quantum algorithmic complexity. Here we would like to compare this briefly to some established proposals of quantum dynamical entropy, such as for example CNT entropy [19] or AF entropy [20], both being ideally suited for a quantum dynamical system formulated in terms of time automorphism \mathbf{T} , tracial invariant state ω , and quasi-local C^* algebra $\mathcal{A}_{\mathbb{Z}}$. We shall here briefly review AF entropy which is conceptually simpler.

Let us start by taking a set of say k elements $A_\alpha, \alpha = 1, \dots, k$ of $\mathcal{A}_{\mathbb{Z}}$ which form a partition of unity, namely $\sum_\alpha A_\alpha^* A_\alpha = \mathbb{1}$. Following the dynamics up to integer time t , $A_\alpha(t) = \mathbf{T}^t A_\alpha$, we construct a set of k^t elements depending on a multi-index $\underline{\alpha} = (\alpha_0, \dots, \alpha_{t-1})$, namely

$$A_{\underline{\alpha}}^{(t)} = A_{\alpha_0}(0)A_{\alpha_1}(1) \cdots A_{\alpha_{t-1}}(t-1) = A_{\alpha_0} \mathbf{T} A_{\alpha_1} \mathbf{T} \cdots \mathbf{T} A_{\alpha_{t-1}}. \tag{45}$$

From the homomorphism property and unitarity of dynamics it follows that $A_{\underline{\alpha}}^{(t)}$ is also a partition of unity, $\sum_{\underline{\alpha}} [A_{\underline{\alpha}}^{(t)}]^* A_{\underline{\alpha}}^{(t)} = \mathbb{1}$. Hence using an invariant state ω one can form a positive, Hermitian, trace-one, $k^t \times k^t$ matrix

$$\rho_{\underline{\alpha}, \underline{\beta}}^{(t)} = \omega([A_{\underline{\beta}}^{(t)}]^* A_{\underline{\alpha}}^{(t)}). \tag{46}$$

$\rho^{(t)}$ can clearly be interpreted as a density matrix pertaining to dynamically generated partition, and its Von Neumann entropy generated per unit time defines the AF entropy

$$S^{\text{AF}} = \sup_{\{A_\alpha\}} \limsup_{t \rightarrow \infty} -\frac{1}{t} \text{tr}[\rho^{(t)} \log \rho^{(t)}], \tag{47}$$

where, strictly speaking, supremum over all possible generating partitions has to be taken. It is not surprising that practical evaluation of S_{AF} is impossible except for rather trivial cases, such as dynamics generated by shift automorphism \mathbf{S}_1 [20]. However, one can easily show that a related linear AF entropy,

$$S_2^{\text{AF}} = \sup_{\{A_\alpha\}} \limsup_{t \rightarrow \infty} -\frac{1}{t} \log \text{tr}[\rho^{(t)}]^2, \tag{48}$$

is tractable much more easily, while the behaviour of S^{AF} and S_2^{AF} is likely to be similar in practice. The key observation is to write the purity $P^{\text{AF}}(t) = \text{tr}[\rho^{(t)}]^2 = \sum_{\underline{\alpha}, \underline{\beta}} \rho_{\underline{\beta}, \underline{\alpha}}^{(t)} \rho_{\underline{\alpha}, \underline{\beta}}^{(t)}$ in terms of dynamics over a product algebra $\tilde{\mathcal{A}}_{\mathbb{Z}} = \mathcal{A}_{\mathbb{Z}} \times \mathcal{A}_{\mathbb{Z}}$, with time automorphism $\tilde{\mathbf{T}}(A \times B) = \mathbf{T}(A) \times \mathbf{T}(B)$ and an invariant state $\tilde{\omega}(A \times B) = \omega(A)\omega(B)$. To this product structure, we add a linear map $\tilde{\mathbf{K}} : \tilde{\mathcal{A}}_{\mathbb{Z}} \rightarrow \tilde{\mathcal{A}}_{\mathbb{Z}}$ depending on a generating partition $\{A_\alpha\}$:

$$\tilde{\mathbf{K}}(\tilde{B}) = \sum_{\alpha, \beta=1}^k (A_\beta \times A_\alpha) \tilde{B} (A_\alpha^* \times A_\beta^*). \tag{49}$$

If $\mathbb{1}$ is a unit element in $\mathcal{A}_{\mathbb{Z}}$ then $\mathbb{1} \times \mathbb{1}$ is a unit element in $\tilde{\mathcal{A}}_{\mathbb{Z}}$, and purity can be written using a transfer-matrix-like approach as

$$P^{\text{AF}}(t) = \tilde{\omega}\{[\tilde{\mathbf{T}}\tilde{\mathbf{K}}]^t (\mathbb{1} \times \mathbb{1})\}. \tag{50}$$

The idea can be worked out in detail for a complete generating partition of a local sub-algebra $\mathcal{A}_{[-q+1, q]}$ of size $k = 4^{2q}$. There it turns out that, due to the locality of dynamics (24), the

resulting purity is *independent* of $q \geq 1$, i.e. the supremum (48) is already achieved by a rather modest partition of $4^2 = 16$ elements, and the map $\tilde{\mathbf{T}}\tilde{\mathbf{K}}$ can be *factored* into a direct product of two maps acting separately on *two independent copies* of a *semi-infinite lattice*. Leaving out some technical details of derivation, the final result reads as follows. Let us consider a time-dependent $4^t \times 4^t$ matrix $Q(t)$, representing a state on $\tilde{\mathcal{A}}_{\mathbb{Z}^+} = \mathcal{A}_{\mathbb{Z}^+} \times \mathcal{A}_{\mathbb{Z}^+}$, with the initial value $Q(0) = Q_{0,0}(0) = 1$, and dynamics given by the following completely positive matrix map:

$$Q(t+1) = \text{tr}_{[0,1]} \{ T_{t+1} [E_{00} \otimes \mathbb{1}_4 \otimes Q(t) \otimes E_{00}] T_{t+1}^\dagger \}, \quad (51)$$

where $(\text{tr}_{[0,1]} R)_{j,k} = \sum_{s=0}^{15} R_{s+16j, s+16k}$ traces out two least important qudits, and unitary time-evolution matrix T_t is given in (41). Then the purity, and linear dynamical entropy (LDE), are simply given as $P^{\text{AF}}(t) = [Q_{0,0}(t)]^2$, $S_2(t) = -2 \log Q_{0,0}(t)$, respectively. The asymptotic increase of $S_2(t)$ per unit time yields the linear AF entropy (48). Again, for practical calculations it is convenient to consider truncation of matrices $Q(t)$ after each iteration (51), say at dimension 4^r . In figure 22, we plot LDE for different cases of KI dynamics, and we observe that LDE is always clearly growing linearly $\propto t$, so the AF entropy is always strictly positive, even in non-ergodic (NE) and integrable (IN) cases, and that the results are robust and stable against changing the truncation order r . Perhaps this finding appears surprising, but one has to bear in mind that AF and CNT entropies can be positive even for simpler dynamics, such as quasi-free flows on C^* algebras.

For *ergodic* dynamical systems on C^* algebras one can use Shannon–McMillan–Breiman (SMB) theorem (for classical SMB theorem see e.g. [78], and [79] for a possible quantum extension), which states that for *typical* sequences $\underline{\alpha}$, a *multi-time correlation function* (MTCF) should decay exponentially

$$C(t) = \omega(A_{\underline{\alpha}}^{(t)}) \sim \exp(-ht), \quad (52)$$

where the exponent h , which should be essentially independent of α , is equal to a dynamical entropy of the map \mathbf{T} with respect to an invariant state ω . For an interesting application of SMB theorem in the context of quantum dynamical chaos see [80]. In our numerical experiments, we considered truncated dynamics $\mathbf{T}_{[-n,n]}$, writing truncation order as $r = 2n+1$, and computed two kinds of MTCF. (i) For a uniform sequence $\underline{\alpha} = (1, 1, \dots)$, where $A_1 = \sigma_0^x$ (or $A_1 = \sigma_0^x \sigma_1^x$ in which case the truncated lattice was placed as $[-n, n+1]$, hence $r = 2n+2$), we estimated MTCF (52) as $(A_1 | \mathbf{T}_{[-n,n]} A_1 \mathbf{T}_{[-n,n]} \cdots \mathbf{T}_{[-n,n]} A_1)$. (ii) For a random sequence $\underline{\alpha}$, we took a complete generating partition $\{|s_{-q}, \dots, s_q\rangle\}$ on $\mathcal{A}_{[-q,q]}$ with $k = 4^l$ elements, for $l \equiv 2q+1 = 1$ or $l = 3$, and computed an average square modulus of MTCF $\langle |C(t)|^2 \rangle = \langle |(A_{\alpha_0} | \mathbf{T}_{[-n,n]} A_{\alpha_1} \mathbf{T}_{[-n,n]} \cdots \mathbf{T}_{[-n,n]} A_{\alpha_{t-1}})|^2 \rangle$ over 20 randomly sampled sequences $\underline{\alpha}$. In both cases (i) and (ii), we have found a rather good agreement between $\log |C(t)|^2$ and LDE $S_2(t)$ for the case of quantum chaotic dynamics (figure 22). For average random MTCF, we found rather good agreement even for non-ergodic cases (NE and IN); however, MTCF for the uniform sequence exhibited big oscillating fluctuations there, indicating simply that SMB theorem does hold for non-ergodic dynamics of the KI model.

Summarizing, it seems that AF entropy, even though it very cleanly generalizes the concept of Kolmogorov–Sinai classical dynamical entropy to quantum dynamical systems, cannot be used as an indicator of quantum chaos or an indicator of computational complexity of quantum dynamical systems. Nevertheless, it has to be stressed that quantum dynamical entropies can be related to the notion of quantum algorithmic complexity, mentioned in section 5, by a quantum version of Brudno theorem established in [81].

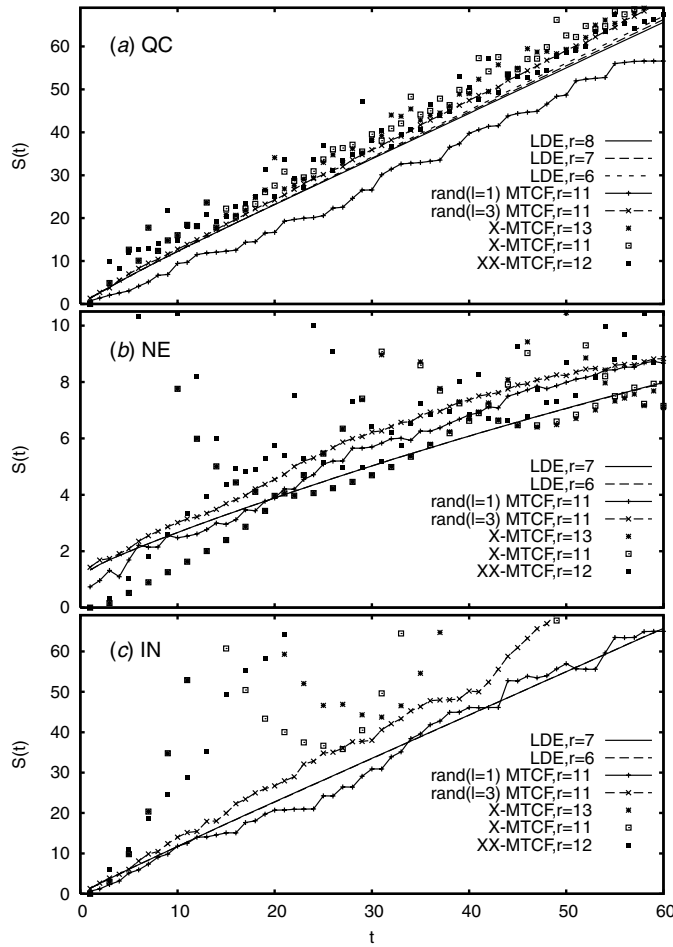


Figure 22. Linear dynamical entropies (continuous curves) for cutoff orders at $r = 6, 7, 8$, for three different cases of dynamics (QC (a), NE (b) and IN (c)), compared to $-\ln|C(t)|^2$ where $C(t)$ are MTCF with observables $X = \sigma_1^x$ and $XX = \sigma_1^x \sigma_2^x$ at different cutoff orders r (symbols), and to average $-\ln(|C(t)|^2)$ over random MTCF sampled over 20 sequences of random Pauli observables of lengths $l = 1$ and $l = 3$ (curve-symbols).

8. Conclusions and open questions

In the present paper, we have reviewed several possible approaches to describe dynamic instabilities, relaxation phenomena and computation complexity in the simple model of one-dimensional non-integrable locally interacting quantum many-body dynamics. We have argued that the essential non-equilibrium statistical properties of quantum dynamical systems—in the absence of idealized external baths—may be crucially related to the integrability of the system, or in the complementary case, to the existence of the regime of quantum chaos.

The general flavour which remains after such studies is that the non-integrable quantum many-body problem at high temperature will preclude any exact and complete solution by its very nature. Still it is hoped that a more complete ergodic theory of such systems could be

developed, allowing for example for exact calculation of relaxation rates, scaling exponents of resonance eigenvectors, etc.

It has been shown in many cases that integrable quantum systems have anomalous non-equilibrium statistical mechanics at high temperature, for example they exhibit ballistic transport. This can easily be understood as being a consequence of the existence of (an infinite sequence of) exact local conservation laws which prevent quantum ergodicity, similarly as the existence of canonical action variables in classical integrable systems prevents classical ergodicity. An interesting open question is as follows. How strong integrability breaking perturbation is needed, in generic cases, to break all the exact conservation laws and yield normal (diffusive) transport? In other words, a quantum KAM theory is needed! Numerical experiments shown in this paper suggest an interesting possibility, namely that in some cases a finite, critical perturbation strength is required.

Acknowledgments

I would like to thank G Casati, T Gorin, C Mejia-Monasterio, T H Seligman, and M Žnidarič, for collaborations on related projects and acknowledge stimulating discussions with F Benatti, J Eisert, S Fishman and P Zoller. This work has been supported by the grants P1-0044, and J1-7347 of Slovenian Research Agency.

References

- [1] Cvitanovic P *et al* 1998 *Classical and Quantum Chaos: A Cyclist Treatise* (Copenhagen: NielsBohr Institute) www.nbi.dk/ChaosBook/
- [2] Haake F 1991 *Quantum Signatures of Chaos* (Berlin: Springer) (2nd enlarged edition 2000)
- [3] Bethe H 1931 *Z. Phys.* **71** 205
- [4] Korepin V E, Bogoliubov N M and Izergin A G 1993 *Quantum Inverse Scattering and Correlation functions* (Cambridge: Cambridge University Press)
- [5] Wilson K G 1975 *Rev. Mod. Phys.* **47** 773
- [6] Foulkes W M C, Mitaš L, Needs R J and Rajagopal G 2001 *Rev. Mod. Phys.* **73** 33
- [7] White S 1992 *Phys. Rev. Lett.* **69** 2863
White S 1993 *Phys. Rev. B* **48** 10345
- [8] Vidal G 2003 *Phys. Rev. Lett.* **91** 147902
Vidal G 2004 *Phys. Rev. Lett.* **93** 040502
White S R and Feiguin A E 2004 *Phys. Rev. Lett.* **93** 076401
Daley A J, Kollath C, Schollwöck U and Vidal G 2005 *J. Stat. Mech.* **4** P04005
Vidal G 2006 *Preprint cond-mat* [0605597](https://arxiv.org/abs/0605597)
- [9] Gobert D, Kollath C, Schollwöck U and Schütz G 2005 *Phys. Rev. E* **71** 036102
Schollwöck U and White S R 2006 *Effective Models for Low-Dimensional Strongly Correlated Systems* ed G G Batrouni and D Poilblanc (Melville, NY: AIP) p 155
- [10] Verstraete F, García-Ripoll J J and Cirac J I 2004 *Phys. Rev. Lett.* **93** 207204
Zwolak M and Vidal G 2004 *Phys. Rev. Lett.* **93** 207205
Feiguin A E and White S R 2005 *Phys. Rev. B* **72** 220401
- [11] Zotos X, Naef F and Prelovšek P 1997 *Phys. Rev. B* **55** 11029
- [12] Berry M V 1991 *Some Quantum-to-Classical Asymptotics (Les Houches Lecture Series LII (1989))* ed M-J Giannoni, A Voros and J Zinn-Justin (Amsterdam: North-Holland) pp 251–304
- [13] Gorin T, Prosen T, Seligman T H and Žnidarič M 2006 *Phys. Rep.* **435** 33
- [14] Casati G, Chirikov B V, Guarneri I and Shepelyanski D 1986 *Phys. Rev. Lett.* **56** 2437
- [15] Jalabert R and Pastawski H M 2001 *Phys. Rev. Lett.* **86** 2490
- [16] Veble G and Prosen T 2004 *Phys. Rev. Lett.* **92** 034101
- [17] Prosen T 2002 *Phys. Rev. E* **65** 036208
- [18] Prosen T 2004 *Physica D* **187** 244
- [19] Connes A, Narnhoffer H and Thirring W 1987 *Commun. Math. Phys.* **112** 691
- [20] Alicki R and Fannes M 1994 *Lett. Math. Phys.* **32** 75

- [21] Benatti F 1993 *Deterministic Chaos in Infinite Quantum Systems (Trieste Notes in Physics)* (Berlin: Springer)
Benatti F, Hudetz T and Knauf A 1998 *Commun. Math. Phys.* **198** 607
- [22] Ablowitz M J and Clarkson P A 1991 *Solitons, Nonlinear Evolution Equations and Inverse Scattering (London Mathematical Society Lecture Notes Series vol 149)* (Cambridge: Cambridge University Press)
- [23] Chirikov B V 1979 *Phys. Rep.* **52** 265
- [24] Prosen T 1999 *Phys. Rev. E* **60** 3949
- [25] Prosen T 1998 *Phys. Rev. Lett.* **80** 1808
- [26] Prosen T 2000 *Prog. Theor. Phys. Suppl.* **139** 191
- [27] Pineda C and Prosen T 2007 *Preprint quant-ph/0702164*
- [28] Peres A 1984 *Phys. Rev. A* **30** 1610
- [29] Veble G and Prosen T 2005 *Phys. Rev. E* **72** 025202
- [30] Guhr T, Müller-Groeling A and Weidenmüller H A 1998 *Phys. Rep.* **299** 189
- [31] Gorin T, Prosen T and Seligman T H 2004 *New J. Phys.* **6** 20
- [32] Cerruti N and Tomsovic S 2003 *J. Phys. A: Math. Gen.* **36** 3451
Cerruti N and Tomsovic S 2003 *J. Phys. A: Math. Gen.* **36** 11915 (corrigendum)
- [33] Frahm K, Fleckinger R and Shepelyanski D 2004 *Eur. Phys. J. D* **29** 139
- [34] Stöckmann H-J and Schäffer R 2005 *Phys. Rev. Lett.* **94** 244101
Stöckmann H-J and Schäffer R 2004 *New J. Phys.* **6** 1999
- [35] Schäffer R, Stöckmann H-J, Gorin T and Seligman T H 2005 *Phys. Rev. Lett.* **95** 184102
Schäffer R, Gorin T, Stöckmann H-J and Seligman T H 2005 *New J. Phys.* **7** 152
Gorin T, Seligman T H and Weaver R L 2006 *Phys. Rev. E* **73** 015202
- [36] Benenti G, Casati G and Montangero S 2003 *Int. J. Mod. Phys. B* **17** 3932
- [37] Levi B, Georgeot B and Shepelyanski D 2003 *Phys. Rev. E* **67** 046220
- [38] Zurek W H 2003 *Rev. Mod. Phys.* **75** 715
- [39] Gorin T, Prosen T, Seligman T H and Strunz W 2004 *Phys. Rev. A* **70** 042105
- [40] Zurek W H and Paz J P 1995 *Physica D* **83** 300
- [41] Miller P A and Sarkar S 1999 *Phys. Rev. E* **60** 1542
- [42] Bandyopadhyay J N and Lakshminarayan A 2004 *Phys. Rev. E* **69** 016201
Jacquod Ph 2004 *Phys. Rev. Lett.* **92** 150403
Petitjean C and Jacquod Ph 2006 *Phys. Rev. Lett.* **97** 194103
- [43] Žnidarič M and Prosen T 2003 *J. Phys. A: Math. Gen.* **36** 2463
- [44] Tanaka A, Fujisaki H and Miyadera T 2002 *Phys. Rev. E* **66** 045201
Fujisaki H, Miyadera T and Tanaka A 2003 *Phys. Rev. E* **67** 066201
- [45] Prosen T and Seligman T H 2002 *J. Phys. A: Math. Gen.* **35** 4707
- [46] Pineda C and Seligman T H 2005 *Phys. Rev. A* **73** 012305
- [47] Prosen T, Seligman T H and Žnidarič M 2003 *Phys. Rev. A* **67** 062108
- [48] Mejia-Monasterio C, Benenti G, Carlo G G and Casati G 2005 *Phys. Rev. A* **71** 062324
- [49] Wang X, Ghose S, Sanders B C and Hu B 2004 *Phys. Rev. E* **70** 016217
- [50] Prosen T and Žnidarič M 2007 *Phys. Rev. E* **75** 015202
- [51] Gacs P 2001 *J. Phys. A: Math. Gen.* **34** 6859
- [52] Vitanyi P 2001 *IEEE Trans. Inf. Theory* **47** 2464
- [53] Berthiaume A, van Dam W and Laplante S 2001 *J. Comput. Syst. Sci.* **63** 201
- [54] Mora C E and Briegel H J 2005 *Phys. Rev. Lett.* **95** 200503
- [55] Osborne T 2005 *Preprint quant-ph/0508031*
- [56] Schumacher B and Werner R F 2004 *Preprint quant-ph/0405174*
- [57] Calabrese P and Cardy J 2005 *J. Stat. Mech.* **04** P04010
De Chiara G, Montangero S, Calabrese P and Fazio R 2006 *J. Stat. Mech.* **5** P03001
- [58] Brandt U and Jacoby K 1976 *Z. Phys. B* **25** 181
Brandt U and Jacoby K 1977 *Z. Phys. B* **26** 245
Perk J H H, Capel H W, Quispel G R W and Nijhoff F W 1984 *Physica A* **123** 1
- [59] Mejia-Monasterio C, Casati G and Prosen T 2005 *Europhys. Lett.* **72** 520
- [60] Kubo R 1957 *J. Phys. Soc. Japan* **12** 570
- [61] Bonetto F, Lebowitz J L and Rey-Bellet L 2000 *Mathematical Physics 2000* vol 128 ed A Fokas, A Grigoryan, T Kibble and B Zegarlinsky (London: Imperial College London)
- [62] Saito K 2003 *Europhys. Lett.* **61** 34
- [63] Michel M, Hartmann M and Mahler G 2003 *Eur. Phys. J. B* **34** 325
- [64] Larralde H, Leyvraz F and Mejia-Monasterio C 2003 *J. Stat. Phys.* **113** 197
- [65] Lindblad G 1976 *Commun. Math. Phys.* **48** 119

- [66] Jensen R V and Shankar R 1985 *Phys. Rev. Lett.* **54** 1879
- [67] Fine B V 1999 *Preprints* cond-mat/9911229
Fine B V 1999 *Preprints* cond-mat/9911230
- [68] Fabricius K, Löw U and Stolze J 1997 *Phys. Rev. B* **55** 5833
Fabricius K and McCoy B M 1998 *Phys. Rev. B* **57** 8340
- [69] Jona-Lasinio G and Presilla C 1996 *Phys. Rev. Lett.* **77** 4322
- [70] Lee M H 1982 *Phys. Rev. Lett.* **49** 1072
Lee M H 1982 *Phys. Rev. B* **26** 2547
Lee M H 2001 *Phys. Rev. Lett.* **87** 250601
Lee M H 2006 *J. Phys. A: Math. Gen.* **39** 4651
Lee M H 2006 *Physica A* **365** 150
- [71] Prosen T 1999 *Phys. Rev. E* **60** 1658
- [72] Bratelli O and Robinson D W 1979, 1981 *Operator Algebras and Quantum Statistical Mechanics I,II* (Berlin: Springer)
Simon B 1993 *The Statistical Mechanics of Lattice Gases* (Princeton, NJ: Princeton University Press)
- [73] Weber J, Haake F and Šeba P 2000 *Phys. Rev. Lett.* **85** 3620
Weber J, Haake F, Braun P A, Manderfeld C and Seba P 2001 *J. Phys. A: Math. Gen.* **34** 7195
- [74] Gaspard P 1998 *Chaos, Scattering and Statistical Mechanics* (Cambridge: Cambridge University Press)
- [75] Grabowski M P and Mathieu P 1995 *Ann. Phys., NY* **243** 299
- [76] Prosen T 1998 *J. Phys. A: Math. Gen.* **31** L645
- [77] Prosen T 2002 *J. Phys. A: Math. Gen.* **35** L737
- [78] Bilingsley P 1965 *Ergodic Theory and Information* (New York: Wiley)
- [79] Bjelaković I, Krüger T, Siegmund-Schultze R and Szkola A 2004 *Inventiones Mathematicae* **155** 203 see also e-print quant-ph 0301177
- [80] Gaspard P 1992 Dynamical chaos in many-body quantum systems *Quantum Chaos—Quantum Measurement* ed P Cvitanović *et al* (Dordrecht: Kluwer) pp 19–42
- [81] Benatti F, Krüger T, Müller M, Siegmund-Schultze R and Szkola A 2006 *Commun. Math. Phys.* **265** 437